공학석사 학위논문

Airway Epithelium-on-a-Chip as a Platform for Particulate Matter Study

미세먼지 세포기전 연구 플랫폼으로써 기도 상피 모사 칩의 개발

2018년 2월

서울대학교 대학원
협동과정 바이오엔지니어링 전공

최 준 희

미세먼지 세포기전 연구 플랫폼으로써 기도 상피 모사 칩의 개발

지도교수 이 정 찬

이 논문을 공학석사 학위논문으로 제출함

2018 년 **1**월

서울대학교 대학원

협동과정 바이오엔지니어링 전공

최 준 희

최준희의 공학석사 학위논문을 인준함

2018 년 **1**월

위 원 장 김 희 찬 **(인)**

부 위 원 장 이 정 찬 **(인)**

위 원 최 영 빈 **(인)**

MASTER THESIS

AIRWAY EPITHELIUM-ON-A-CHIP AS A PLATFORM FOR PARTICULATE MATTER STUDY

BY

CHOI JUN HEE

FEBRUARY 2018

INTERDISCIPLINARY PROGRAM IN

BIOENGINEERING

THE GRADUATE SCHOOL

SEOUL NATIONAL UNIVERSITY

Airway Epithelium-on-a-Chip as a Platform for Particulate Matter Study

Academic adviser **Jung Chan Lee**
Submitting a master's thesis of Engineering
January 2018

Interdisciplinary Program in Bioengineering
Graduate School, Seoul National University

Jun Hee Choi

Confirming the master's thesis written by Jun Hee Choi
January 2018

Chair _____

Hee Chan Kim, Ph.D.

Vice Chair _____

Jung Chan Lee, Ph.D.

Examiner _____

Young Bin Choy, Ph.D.

Abstract

Airway Epithelium-on-a-Chip as a Platform for Particulate Matter Study

Junhee Choi
Interdisciplinary Program in Bioengineering
Seoul National University Graduate School

The purpose of this research is to develop a microfluidic Airway Epithelium-on-a-Chip, a novel *in-vitro* model for assessing effects of particulate matters (PM) on airway epithelium, and to evaluate its potential as a platform for PM study. The characteristic of human airway, which is the consecutive connection of different epitheliums, is established on upper channel of the chip, using a novel microfluidic cell-culture method. As airway epithelium is formed, on-chip cultured cells were exposed to diesel exhaust particles (DEP), and as a consequence, EMT (Epithelial-to-Mesenchymal Transition) and inflammatory reaction were observed on chip. In order to examine functionality and reliability of the chip, DEP experiments on cell culture plate and animal model are conducted. For animal model, asthma-induced mouse is used.

Airway Epithelium-on-a-Chip is made of PDMS (Polydimethylsiloxane) and consisted of the upper channel, which enables in-series culture of different epithelial cells, ECM (Extra-cellular matrix)-coated membrane, and the lower channel, in which continuous perfusion is made. To mimic airway epithelium, human nasal epithelial cell line and human alveolar epithelial cell line are used and cells are co-cultured in-series. Moreover, fibronectin is coated

on porous PET membrane in order to support cell attachments and proliferation. In order for long-term survival of on-chip cultured cells, the lower channel is connected to a syringe pump, which makes continuous flow of media.

The confluency of two epithelial cells cultured inside the chip is observed using daily microscopic images and the epithelialization is verified by the formation of tight junctions between cells. Also, as the epithelial cell layer is exposed to sonicated DEP, the EMT ability and the release of pro-inflammatory cytokines are investigated using immunofluorescence staining and PCR (Polymerase Chain Reaction). To verify the on-chip results, in-vitro experiment and in-vivo study using asthma mouse are conducted simultaneously. During in-vitro experiment, human alveolar epithelial cells (A549) are cultured on cell culture plate and exposed to DEP and TGF-beta, and the formation of tight junctions and EMT ability are compared between control and experimental groups. During in-vivo study, an asthma-induced mouse is treated with DEP for 3 days using intra-nasal challenges and sacrificed. Its lung cells are then gone through PCR for investigating the secretion of inflammatory cytokines.

Cells cultured inside the chip formed tight junctions in 2 days and achieve the full confluency in 4 days. As effects of DEP on epithelial cells, the breakage of tight junction, increased EMT ability and the secretion of IL-6 were observed. Significant similarity was found between on-chip results and those from in-vitro and in-vivo experiments. *In vitro* experiments resulted in the breakage of tight junctions and increased EMT ability of epithelial cell layers, while *in vivo* experiments resulted in the elevated level of IL-6 mRNA from DEP-treated asthma mouse model.

In this study, a microfluidic airway epithelial chip was developed and tested for its reaction to Diesel Exhaust Particles. The formation of tight junction and gradual increase of cell layer in microscopic images prove the formation of epithelium on the chip, which also verifies the functionality of Airway Epithelium-on-a-Chip. Moreover, the elevation of IL-6, known

inflammatory cytokine, was observed on the chip, which was supported by the in-vivo mouse model. By showing the agreement between on-chip results and in-vivo results, the reliability of the microfluidic chip has been assured.

Organ-on-a-Chip is an emerging 3D in-vitro model, which can provide tissue-level functions by reconstructing minimal functional units of organs. Applying this concept, Airway Epithelium-on-a-Chip is developed as a novel in-vitro model that mimics the consecutive lining of airway epithelium. The novel microfluidic in-series co-culture technique, introduced in this research, can be further applied to study interactions of different epithelium. For instance, the consecutive lining of intestinal epithelium can be mimicked using this microfluidic channel design. Further plans should be made to address limitations from this research. In order to improve the functional and environmental similarity to real tissue, the use of primary cells and their differentiation inside the chip are inevitable. Moreover, other air pollutants than DEP should be tested for enhancing the functionality of the chip. Despite these needs for further studies, however, this research clearly implies the potential of Airway Epithelium-on-a-Chip to be a platform for investigating underlying cellular mechanisms of PM.

Keywords: Airway Epithelium-on-a-Chip, Organ-on-a-Chip, Particulate Matters (PM), Diesel Exhaust Particles (DEP),

Student Number: 2016-21181

Table of Contents

List of Tables

List of Figures

List of Abbreviation

PM	Particulate Matter
DEP	Diesel Exhaust Particles
EMT	Epithelial-to-Mesenchymal Transition
PDMS	Polydimethylsiloxane
ECM	Extra-Cellular Matrix
TEER	Trans-Epithelial Electrical Resistance
PET	Polyethylene terephthalate
PCR	Polymerase Chain Reaction

Chapter 1. Introduction

1.1 Research Background

1.1.1 Issues on Particulate Matters

Particulate matter (PM) is a complex mixture of micro-sized particles and droplets suspended in air, including particles like dust, pollen, smoke, and other inorganic particles [1]. The size, chemical composition, and other physical and biological properties of particles vary with location and time and they can be either directly emitted or indirectly formed. For instance, particles can be formed from burnt fuel and carried wind, or from emitted pollutants. Particulate matter is often classified into three groups based on its diameter; coarse (aerodynamic diameter < 10 um), fine (d < 2.5 um) and ultrafine (d < 0.1 um) [2]. To simplify, these groups are commonly indicated by PM_{10}, $PM_{2.5}$, and $PM_{0.1}$, respectively (Figure 1.1). The size is to be the key property of PM for it indicates its capacity to penetrate into the human respiratory system, and even, in worst scenario, into the capillary.

Because of its adverse health effects and deterioration in quality of daily lives [3-7], PM has become a major public health concern today. Not only pulmonary and cardiovascular diseases, crucial brain damage by air pollutants was even reported in literature [8]. Strikingly, studies on the correlation between mortality and PM concentrations also showed that chances of death increase with more exposure to air pollutants [7, 9-10]. Even more, the recent study of Hwang et al. showed that respiratory and cardiovascular ER visits are associated with PM components in South Korea [6]. For these reasons, PM was designated as the primary cancer-

causing agent by International Agency for Research on Cancer (IARC). According to World Health Organization (WHO), approximately 3% of cardiopulmonary and 5% of lung cancer deaths are attributable to PM globally [11]. Another study reports that exposure to $PM_{2.5}$ decreases the life expectance of the population by about 8.6 months in average [12].

As the effects of PM on human health are severe, there have been many approaches to reduce the ambient PM concentrations [13]. However, despite recent improvements of air quality in European region, efforts have not been come to fruition in most Asian countries [14-15]. Due to rapid industrialization and globalization processes such as increased transportations, building structures and combusting in power plants, the concentrations of air pollutants in East Asia countries have been increased [14-16]. In particular, as South Korea has undergone a drastic progress in industrialization and globalization over the past 60 years, the significant deterioration of air quality has been reported with the dramatic increase in concentration of PM in South Korea [17-18]. Moreover, the polluted air from factories in China has been continuously brought into the west side of South Korea for few decades [16]. As a result, the study of Sharma et al., where PM_{10} concentrations in major cities of South Korea were investigated for 14 years [17], indicates that concentrations of PM_{10} in any cities in South Korea are significantly larger than those guided by WHO. Figure 1.2 also points out the danger of increased PM concentration in Seoul, South Korea.

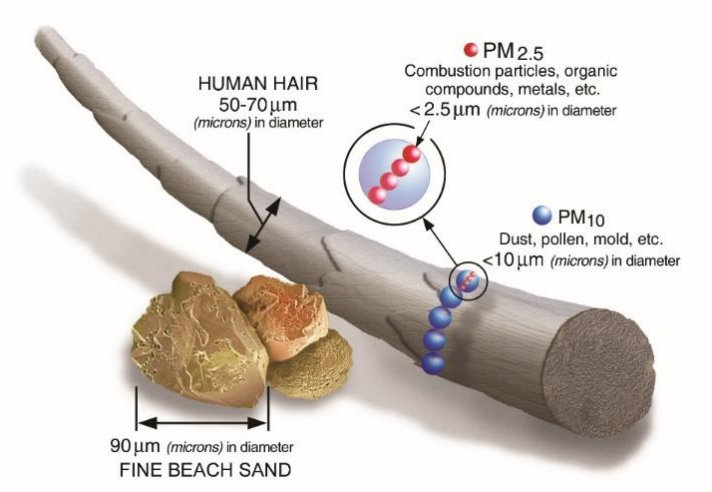

Figure 1.1 Size comparisons for particulate matter (PM). The size of PM is far smaller than that of fine beach sand and human hair. PM_{10} indicates particles with diameter that are generally 10 micrometers and smaller and $PM_{2.5}$ indicates those less than 2.5 micrometers. This image is adapted from U. S. EPA [2].

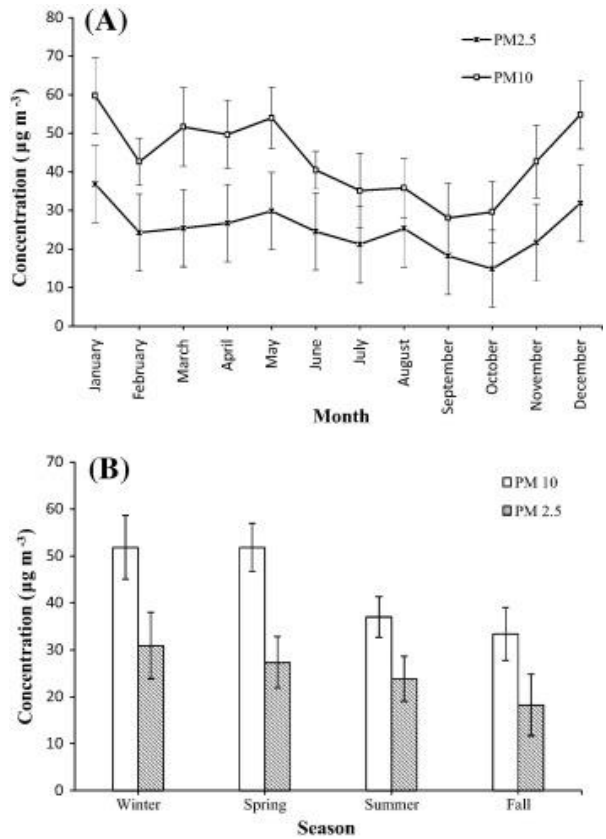

Figure 1.2 Concentrations of PM_{10} and $PM_{2.5}$ at Yongsan-gu, Seoul, South Korea. (A) Temporal variations of PM across months and (B) seasons. Note that despite comparably large variations, mean values of PM_{10} on every month and season are higher than that from WHO guideline, which is 20 $\mu g/m^3$. Likewise, mean values of $PM_{2.5}$.5 on every month and season are higher than WHO guideline, 10 $\mu g/m^3$. This graph is adapted from Vellingiri, et al. [18].

1.1.2 Diesel Exhaust Particles (DEP)

Among many different PM components, a diesel exhaust particle (DEP) is infamous for its omnipresence in the environment [19]. The origin of DEP is mostly the diesel engine, which is the most popular of all existing internal combustion engines. For their use in transportation, the use of diesel engines had raised dramatically in decades, resulting in drastic increase of DEP exposure in the ambient air [20]. Transportation with diesel engines without filters emit up to 100 times more particles compared to that with gasoline engines equipped with filters. The particles produced by diesel engines are often between 10 and 30 nm but they have a tendency to agglomerate, forming a random diameter ranging from 1 to 10 μm [19]. The outer shell of DEP is known to contain metals, such as copper or zinc and a multitude of polycyclic aromatic hydrocarbons (PAHs), such as anthracene or benzo(a)pyrene [19].

The toxicity of DEP is from their constant contact with the respiratory tract and due to its small size, DEP is able not only to stress nasal region, also to reach the alveolar region on human airway [21]. A large number of toxicological studies clearly show that diesel engine emissions profoundly affect human health [21-24]. Similar to the effects of PM on human health, those of DEP include cancer-inducing, inflammation on respiratory system and lung functions.

1.1.3 Effects of Particulate Matters on Human Airway

The role of respiratory system is to provide sufficient oxygen into body and take out carbon dioxide as waste, which makes human breath continuously. When human breathes outside, PM is inhaled, targeting airway epithelium. Although a large part of inhaled PM normally gets entrapped and eliminated by mucociliary escalator and surfactant secreted by epithelium from nose to alveolus, some, in the worst case, would reach to deeper side of respiratory tract, depositing into epithelium. The particles deposited in alveolar region may damage lung epithelial cells and even penetrate into blood vessels near lung tissues. This phenomena can result in many deteriorating health effects, leading to severe lung diseases [19, 21-25, 27].

The deposition of particles on human respiratory tract depends on its diameter (Figure 1.3). When particles' diameter is around 10 μm, they are filtered by nasal epithelial cells. As it gets smaller until 2.5 μm, particles would deposit into bronchus epithelium. If it even decreases to less than 1 μm, particles are likely to deposit into alveolus, where it can attack cell membrane and affect DNA transcriptions [25].

The most evident and basic effect of PM on human airway epithelium is epithelial inflammation [27-28]. Inflammation is a biological response of body tissues to harmful stimuli, such as foreign materials, pathogens, allergens, damaged cells and so on. The main role of inflammation is to protect the stimulated region by eliminating the initial cause of cell injury. It also clears out necrotic cells and damaged tissue areas and initiates tissue repair. When particles are inhaled and deposit into airway, they attack epithelial cells they sit on. Cells recognize particles as external injuries, which becomes the initial step of inflammation [29].

There have been many studies examining the effects of DEPs that report signs of airway inflammation [28-30]. The signs include mucus hypersecretion, increased expression of

pro-inflammatory cytokines, and increase of disease-fighting white blood cells, such as eosinophils, neutrophils, and lymphocytes [28-30]. Similarly, there have been many in-vitro studies using airway epithelial cells, which supported pro-inflammatory capacity of DEP [32-33]. Increased reactive oxygen, increased cell signaling, increased RNA level and release of pro-inflammatory mediators were found as signs of inflammation [27-29, 32-33].

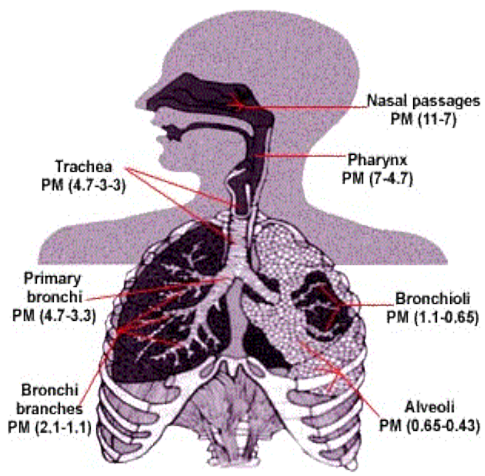

Figure 1.3 Deposition of particles based on their diameter in the respiratory system. Note that as the diameter of particles decrease, particles tend to deposit in deeper side of respiratory tract. Particles whose diameters are less than 0.65 can deposit on alveoli surface, causing cellular damage. This image is adapted from the work of Richard Wilson [26].

1.2 Research Needs

As introduced in sections above, many in-vitro and in-vivo models have been conducted to investigate effects of PM on airway tissues and epithelial cells. To explore further than the superficial effects of PM, studies on underlying cellular and molecular mechanisms of PM on airway epithelium have acquired recent attentions. However, although many important findings had been made from both conventional in-vitro and small animal in-vivo models, there have been many challenges in terms of research efficiency [34]. In-vitro models, while providing comparably easy and cheap experiments using cell-culture plates, are difficult to mimic microenvironment of cells. In this manner, concerns on reliability can be aroused. On the other hand, in-vivo models can reduce the uncertainty of in-vitro models and provide interactions among different systems, despite its high cost and concerns on the gap between human and other animals.

In order to overcome challenges of both in-vitro and in-vivo models, 3D in-vitro models have emerged as they can imitate microenvironments of cells in 3D. These models have been used in reconstructing 3D structure of human airway tissue, which helps to uncover the underlying cellular and molecular mechanism of PM in human airway [35-37]. One of emerging 3D in-vitro technologies is Organ-on-a-Chip, in which minimal functional units of organs are reconstructed to provide tissue-level functions.

Organ-on-a-Chip technology is based on microfluidics, culturing living cells on extra-cellular matrix (ECM)-coated membrane in continuously perfused, micro-sized channels [34]. To fabricate biocompatible microfluidic channel, soft lithography method is used [38]. By culturing living cells of interest in microchannel, physiological functions of tissues can be modeled [39-46]. Organ-on-chips are usually made of two layers of PDMS slab separated by an ECM-coated membrane, each layer containing a microfluidic channel for cell culture. Using

two layers and a membrane, they can provide more physiological human tissue modeling. For instance, when lung epithelial cells are cultured on one side of membrane and endothelial cells are cultured on the other side, the cross-section of alveolar tissue can be remodeled (Figure 1.5). Also, by giving a cyclic strain to the chip, it can also mimic the mechanical stress that human alveolus experience [39]. Table 1.1 shows the multiple studies on imitating human organs using Organ-on-a-Chip technology, where Lung-on-a-Chip has been the pioneering work. Recent researches have shown that microfluidic cell culture systems outperform conventional cell culture and assay systems and bring more reliable results due to their ability to grow cells as in biological systems [34]. Not only they excel in imitating tissue physiology, but they are easy to handle, fabricate and reproduce, which are important assets of a platform for biological studies. For these reasons, this technology has potential to become a platform for determining basic mechanisms of organ physiology and disease.

Name of device	Target Organs (Tissue)	Published Year
Lung-on-a-chip [39]	Human Alveolus	2010
Gut-on-a-chip [40]	Human Gut	2012
Placenta-on-a-chip [41]	Human Placental barrier	2016
Kiney-on-a-chip [42]	Proximal tubule	2013
BBB-on-a-chip [43]	Brain-blood barrier	2013
Liver-on-a-chip [44]	Immune Protected Liver tissue	2015
Vasculature-on-a-chip [45]	Sprouting blood vessels	2016
Heart-on-a-chip [46]	Beating heart culture	2015

Table 1.1 Recent Organ-on-chips studies. There have been many studies on reconstituting organ-level functions on a PDMS microfluidic chip. Many target organs, even blood vessels, have been successfully mimicked as novel in-vitro models.

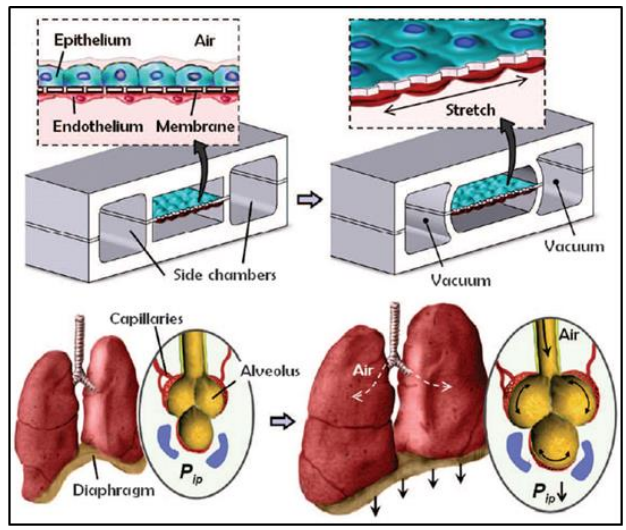

Figure 1.4 Schematic of Lung-on-a-Chip. Alveolar epithelial cells are cultured on collagen-coated membrane and endothelial cells are cultured on the other side of the membrane. Along with microfluidic cell culture, periodic stretch is made using microfluidic vacuum channels, imitating the cyclic strain of lung that alveolar cells experience during normal breath. This image is adapted from Huh et al. [39].

1.3 Research Aims

The aim of this research is to build Airway Epithelium-on-a-Chip, using a new microfluidic cell culture method of culturing two different cell types on one channel. Consequently, the final goal of this research is to define Airway Epithelium-on-a-Chip as a platform for assessing the cellular mechanisms of PM on human airway epithelium. The microfluidic channel was designed to culture two different airway epithelial cells in one channel. For imitating human airway epithelium, human nasal epithelial cell line and human alveolar epithelial cell line were co-cultured on fibronectin-coated membrane, provided with continuous perfusion using a syringe pump. The entire device is made of PDMS (Polydimethylsiloxane), which provides great gas permeability, biocompatibility and reproducibility [34]. To verify the functionality of the chip, on-chip cultured cells were allowed to proliferate until full confluency and exposed to DEP. As effects of DEP on epithelium, the EMT (Epithelial-to-Mesenchymal Transition) ability and the secretion of pro-inflammatory cytokines were observed. The reliability of on-chip results was also assured by conducing conventional in-vitro study and in-vivo mouse model study.

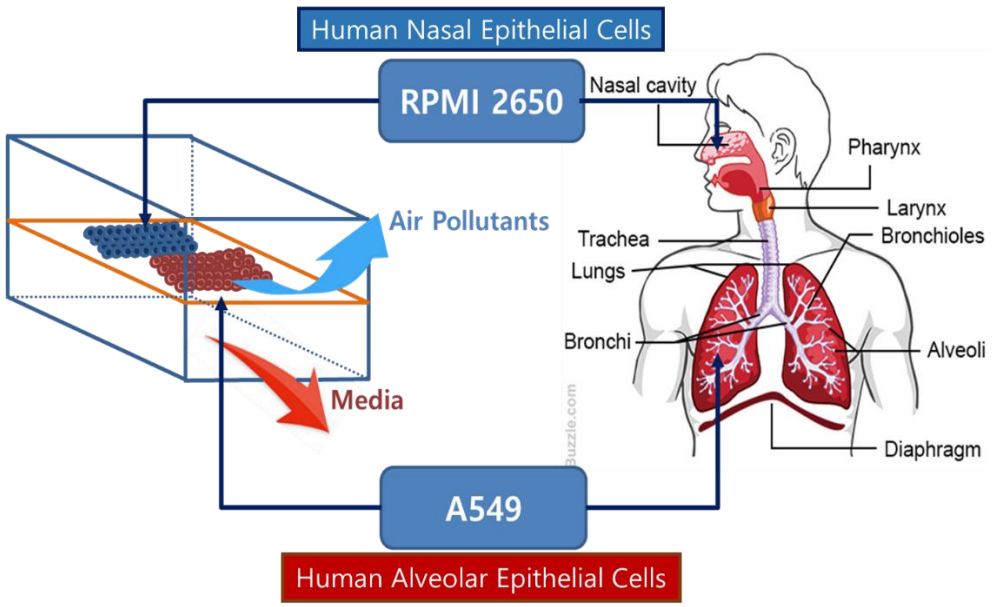

Figure 1.5 Schematic of a microfluidic Airway Epithelium-on-a-Chip. Two different types of airway epithelium, A549 and RPMI2650 are cultured in series, in order to mimic human respiratory tract. This system is then used to evaluate the effect of Diesel Exhaust Particles on airway epithelium.

Chapter 2. Methods

2.1 Device Design and Fabrication

A microfluidic Airway Epithelium-on-a-Chip was made of two flexible clear polydimethylsiloxane (PDMS) (Daehan Science, Korea) polymer slabs and one porous membrane. The PDMS slabs with microchannel patterns were fabricated by casting PDMS polymer on the silicon master mold. The fabrication process of the silicon mold, known as soft lithography, is briefly introduced in Figure 2.1 [34]. For simple explanation, a negative photoresist (PR) (SU-8) was spin-coated on a clean silicon wafer, which was then overlaid with a photomask film containing the designed microchannel patterns [38]. The photomask film only protects the microchannel patterned region of the photoresist from ultraviolet (UV) exposure, while leaving others dissolved in a developer solution. This process provides the clean silicon mold containing the positive relief of the designed microchannel (Figure 2.1).

The microfluidic channels were designed using the computer-aided design software, AutoCAD (Autodesk, USA). A CAD image of the upper and lower layers of the microfluidic device is shown in Figure 2.2. The cross-sectional size of the microchannel is 8 mm × 400 μm for the culture area. Various parameters of the microfluidic chip, including channel size, shape, and bubble formation, can affect cell confluency, the microfluidic Airway Epithelium-on-a-Chip has been undergone some design changes (Figure 2.3). One important design consideration was the presence of the electrode channels, which were meant to measure trans-epithelial electrical resistance (TEER) values of cell culture. However, as air bubbles were

constantly trapped in the electrode channels, they affect both cell confluency and TEER values, resulting in unreliable results. Therefore, the electrode channels were excluded from the design consideration and the width and length of channels were become longer and shorter, respectively, to ease cell proliferation. Another important design consideration was to make two type of cell culture in-series possible. This was fulfilled by making side channels branching from central channel (Figure 2.2). The detailed procedure for culturing two different cells in one channel is presented in Microfluidic Cell Culture section of Methods.

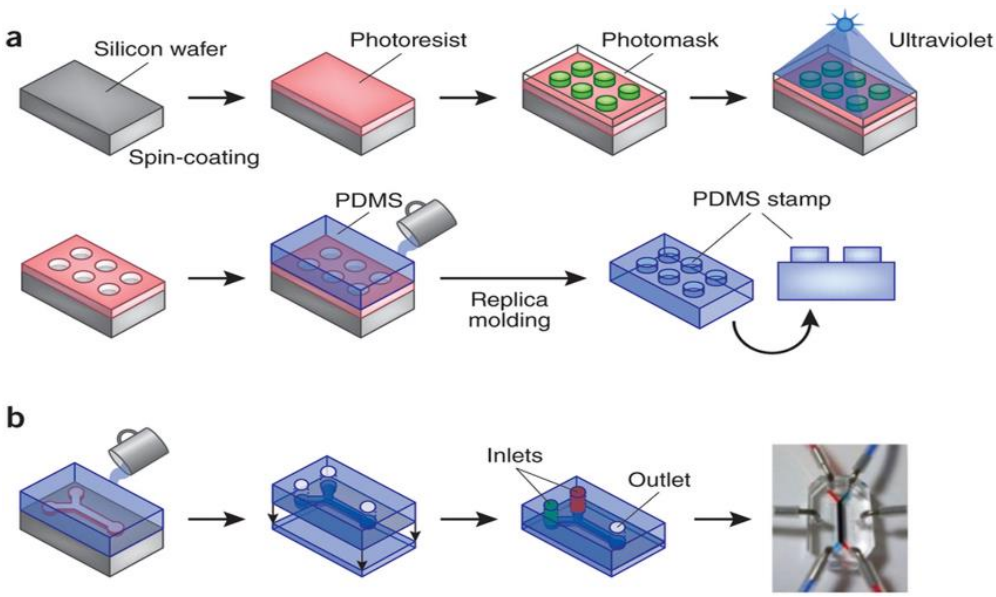

Figure 2.1 Fabrication methods of organ-on-chips. a. Soft-lithography technique. A thin uniform film of photoresist is spin-coated on a silicon wafer, overlaid by a photomask with the desired microscale pattern. Exposing the photomask to UV lead to the microscale pattern etched into the photoresist. b. PDMS mixture (10:1 wt.) is poured on the silicon mold and baked in oven at 60℃ overnight. Inlets and outlets of replicated PDMS slab are punched to connect tubes for continuous perfusion. This image is adapted from Ingber et al. [38].

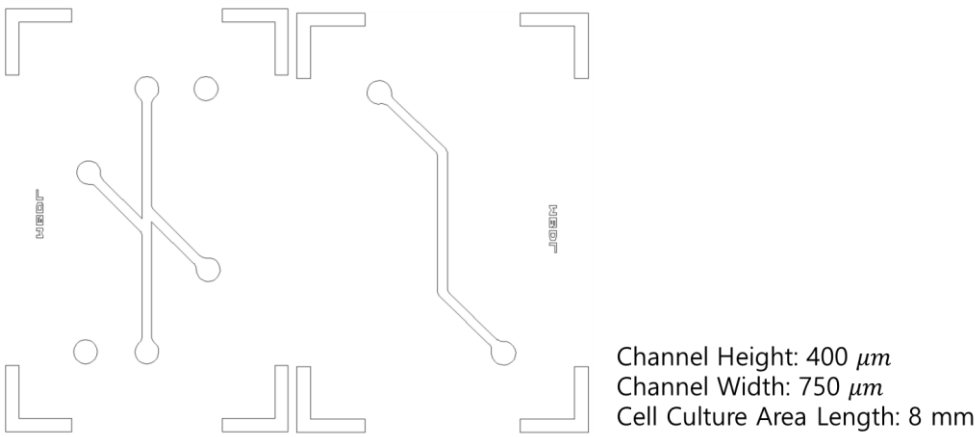

Figure 2.2 Design of upper and lower channels. (Left) a center channel has two branching channels for in-series co-culture of two different cells. Two circles are outlets of lower channels, where media is perfused. (Right) a continuous channel is designed for continuous perfusion. When assembled, lower channel provides cell media to only central region of the upper channel. Width and height of the channel are 750 μm and 400 μm, respectively.

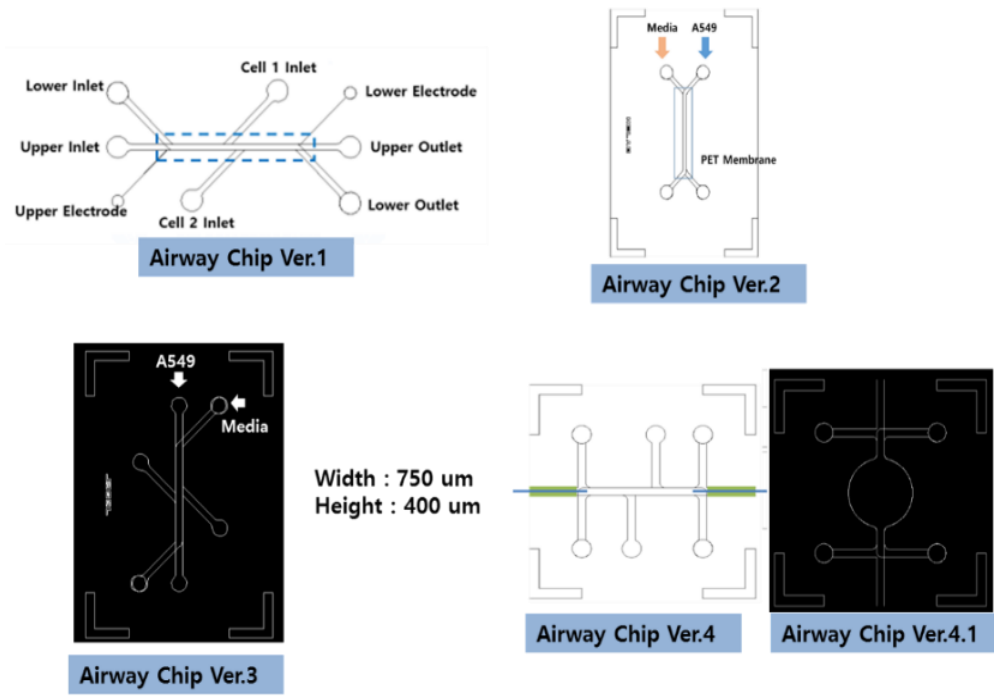

Figure 2.3 Chip design modifications (Ver.1 to Ver. 4.) Ver.1 is designed with electrode channels, for measuring TEER. Ver. 2 is designed for single cell culture. Ver.3 is designed without electrode channels and smaller cell culture area. Ver.4 and Ver.4.1 are designed for horizontal insertion of electrodes. Ver. 3 is selected for developing Airway Epithelium-on-a-Chip.

To create PDMS slabs, PDMS mixture was made using the weight ratio of PDMS base to curing agent (10:1). PDMS mixture was then vacuumed for 30 minutes (or more if necessary) to remove trapped air bubbles. The mixture was gently poured in the silicon mold, and overnight baking at 60°C in the oven. Here, extreme care was taken to keep the wafer parallel to the ground. The cured, rubber-like PDMS was cut into a rectangular block, keeping microchannel located at the center of the rectangle. Inlet and outlets of channels were punched using biopsy puncture (Kai medial, Germany) on upper PDMS slab. Note that none is punctured on lower PDMS slab. To keep the surface clean, the slabs were taped until the assembly. The PDMS channels were separated by a thin porous Polyethylene terephthalate (PET) membrane (0.4 μm pores) (SPL Life Sciences Co., Pocheon, Korea), which was cut from 6-well transwell inserts.

Upper and lower PDMS slabs and the membrane were plasma-treated using Plasma Etcher (Harrick Plasma, NY, USA) for 1 minute at high RF level for irreversible bond. If the device needs to be disassembled later on, plasma-treating for 30~60 seconds at low RF level is recommended. For complete alignment of the upper and lower channels, a light microscopy was used. As shown in Figure 2.4, PET membrane was sandwiched between the upper and lower channels. The assembled device was then put into 60°C oven overnight for complete bonding.

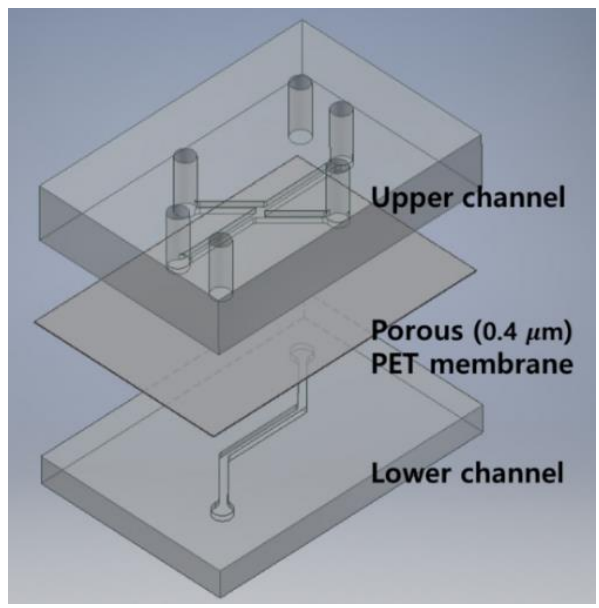

Figure 2.4 Assembly of Airway Epithelium-on-a-Chip. Each fully cured PDMS slab (upper and lower) is cut into a rectangular block and surface-treated with oxygen plasma. The porous PET membrane is sandwiched between two slabs and bonded.

2.2 Microfluidic Cell Culture

Human nasal epithelial cell line (RPMI 2650) and human alveolar basal epithelial cell line (A549) were used in this study. All cells were prepared from Laboratory of Mucosal Immunity, Biomedical Science department of Seoul National University of Medicine. A549 and RPMI2650 were cultured in cell-culture plate and they were grown in RPMI medium, supplemented with 10% FBS. The cells were maintained at 37℃ in a humidified incubator under 5% CO_2 in air. 7 or 8 cell passage number was used for microfluidic cell culture.

Before cell seeding, microfluidic cell culture chips were sterilized by UV irradiation for 1 hour, and the porous membranes were coated with fibronectin. The cells were then seeded into the upper channel at 5×10^4 cells/mL and allowed to attach to the membrane surface for 2-4 hours under static conditions. Figure 2.5 shows the detailed protocol for seeding two different types of cells on the upper channel. RPMI2650, which showed slower proliferation rate than A549, was seeded first and about 6-12 hours were given before seeding A549 on the chip.

About 2-3 hours later, when cells were attached on the upper channel of the chip, the cell layer was washed with fresh medium, and perfused with culture medium by a syringe pump (KD scientific, USA) at a volumetric flow rate of 50 μl/hr. Tubes and 3 mL syringe were used to connect the chip to a syringe pump. The cells in upper microchannel were grown to fill the entire channel within 3 to 4 days. The cells cultured in a microfluidic chip were maintained at 37℃ in a humidified incubator with 5% CO_2 in air (Figure 2.6).

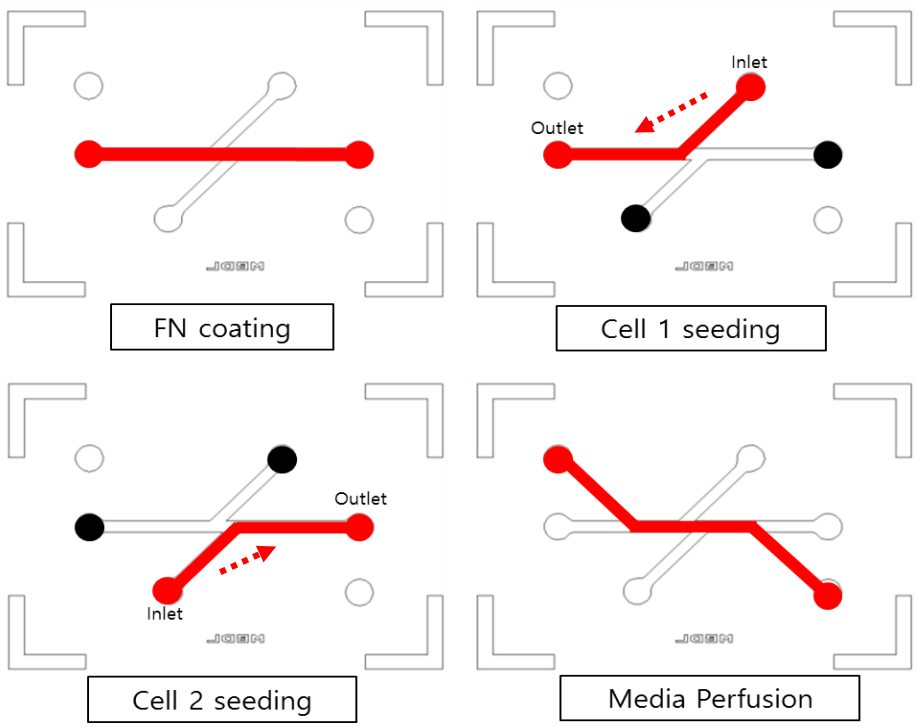

Figure 2.5 Protocol for in-series co-culture of two different cells. Red dots indicate opened inlets and outlet while black dots indicate blocked outlets. Red lines and arrows mean perfusion and its direction, respectively. First, a central channel of upper microfluidic channel is coated with fibronectin. Then, cell 1 is seeded from one side branch to the central channel, while blocking outlets to prevent immersion of cell fluids in undesired region. Similarly cell 2 is seeded from the other side branch to the central channel. Finally, cellular media is perfused in a lower channel.

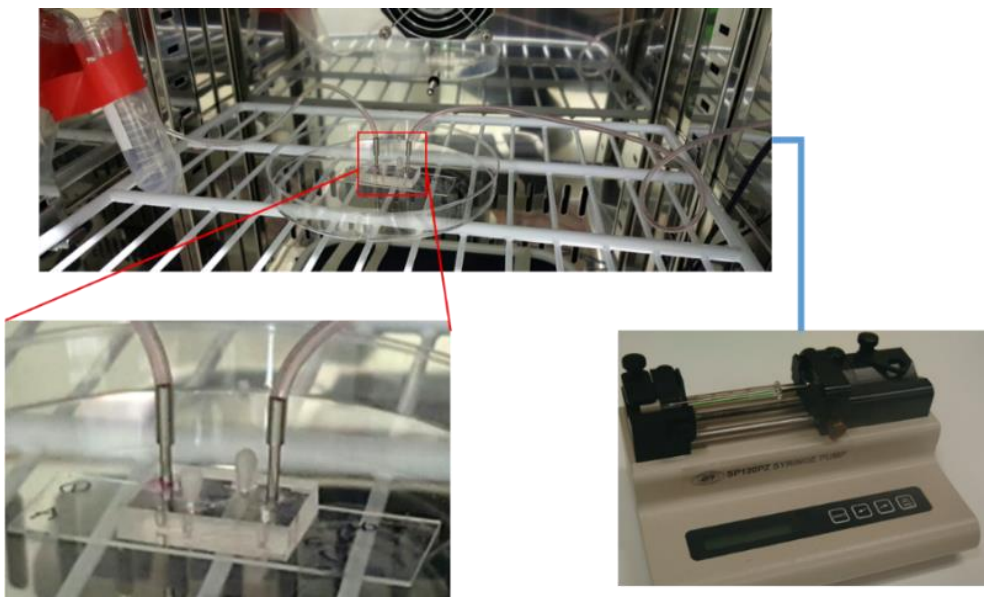

Figure 2.6 Incubation and perfusion of Airway Epithelium-on-a-Chip. One Airway Epithelium-on-a-Chip is connected to a syringe pump for continuous perfusion of media. It is incubated at 37℃ in a humidified condition with 5% CO_2 in air during entire experiments.

2.3 Immunofluorescence Staining

To evaluate the formation of tight junction between cultured epithelial cells on the chip, immunofluorescence staining was held. Cells were grown on the microfluidic chip and exposed to DEP for 48 h. After washing with PBS, the chip was disassembled and cells were fixed in 4% paraformaldehyde (Biosesang, Seoul, South Korea) for 15 min at room temperature. Fixed cells were permeabilized for 30 min at 37°C with Triton X-100 in PBS and then blocked for 1 h at room temperature with 3% bovine serum albumin (BSA) in PBST (PBS + 0.5% Tween 20). Cells were incubated overnight at 4°C with primary antibody (α-SMA and E-cadherin). After washing with PBST, cells were then stained with the Alexa 488-conjugated donkey anti-rabbit IgG (for E-cadherin) and Alexa 555-conjugated donkey anti-mouse IgG (for α-SMA), which were diluted in PBST with 1% BSA. For immunofluorescence staining of tissues, Alexa 555-conjugated donkey anti-mouse IgG (for IFN-γ), Alexa 488-conjugated donkey anti-rabbit IgG (for E-cadherin), and Alexa 488-conjugated donkey anti-rabbit IgG (for neutrophil elastase) were used as primary antibodies. To visualize the nucleus, cells were incubated with 4′,6-diamidino-2-phenylindole (DAPI) (Sigma-Aldrich, St. Louis, USA). An irrelevant isotype antibody was used as a negative control. The slides were covered with mounting medium (Dako, Santa Clara, USA). Cells were analyzed using an inverted laser-scanning microscope (Carl Zeiss Microscopy, Göttingen, Germany). The images were scanned under a ×40 or ×100 oil immersion objective. Co-localization of target proteins was analyzed using Zeiss confocal software (ZEN Lite, Göttingen, Germany).

2.4 Image Acquisition and Analysis

Olympus CK2 (x100) light microscope was used to observe confluency of cells seeded on a chip. Images were acquired from the microscope at each day of cell culture, setting day 0 as the day of cell seeding. Day 1 represents the day after seeding. Acquired images were then processed according to the algorithm shown in Figure 2.7 using Matlab (Mathworks, Inc. USA). This algorithm was used to determine the region of interest in the microscopic images and to convert images into binary images, which makes it easier to evaluate the regional difference between images. It is assumed that as cells proliferate, they cover more region of the upper channel of chip. This assumption is based on the microscopic observations. Therefore, the increase of white region in the binary image indicates more confluency of cells cultured on chip.

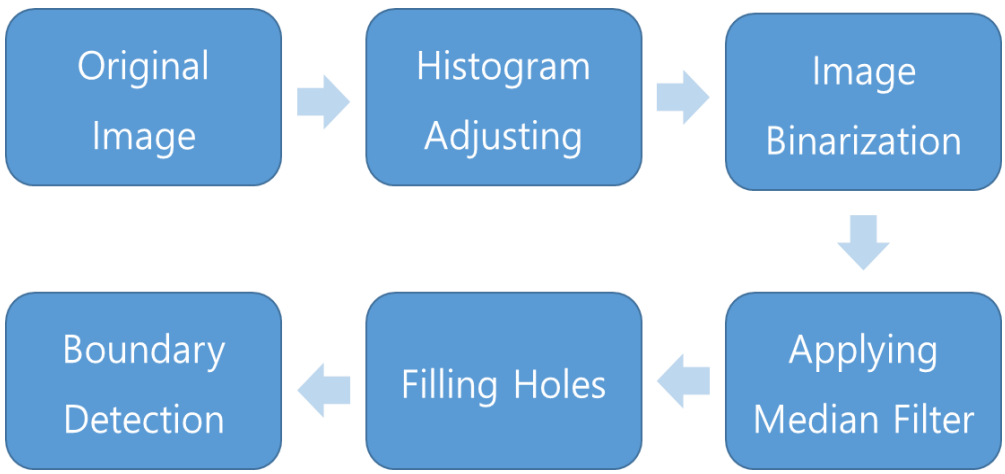

Figure 2.7 Simple diagram for image processing algorithms. Histograms of original microscopic images are adjusted and images are binarized for easy managing. Noise is removed using median filter. Cell culture area in binarized images is revised with hole-filling methods. The boundary of final images is detected.

2.5 Diesel Exhaust Particles Exposure and PCR Analysis

To evaluate the effect of DEP on airway epithelium formed inside the chip, DEP was exposed to upper channel of the chip, using micropipette. Figure 2.8 shows the flow diagram of DEP exposure on the chip. Before treating, DEP was sonicated to make agglomerates into micro particles. Sonication was performed more than 10 minutes using Vibra-Cell (Sonics, USA). 50 μL of prepared DEP was then exposed to the fully proliferated epithelium of the chip. The day after, cells inside the upper channel were treated with TRIzol to extract RNA from cells. Extracted cells were gone through qPCR using CFX Connect Real-Time PCR (Bio-Rad, South Korea)

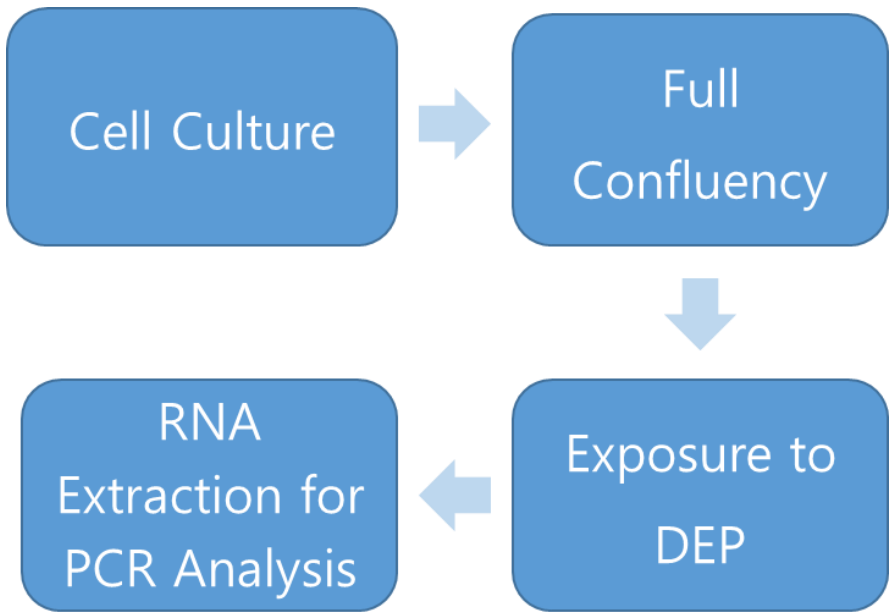

Figure 2.8 Simple diagram of experimental procedure for DEP exposure on Airway Epithelium-on-a-Chip. Cells are allowed to proliferate for 3-4 days until full confluency and exposed to DEP. A day after, RNA of DEP-treated cells are extracted and undergone for PCR.

2.6 DEP Exposure on Cell-Culture Plate

A549 (Human alveolar epithelial cell line) was cultured on a conventional cell-culture plate and allowed to proliferate until over 90% confluency was achieved. Cells were then exposed to different amount of DEP (20 μg and 50μg) and TGF-beta. TGF-beta, transforming growth factor beta superfamily of cytokines, is a known strong EMT inducer, which, in this experiment, is used as a comparison. 50 μg of TGF-beta with 20 ng/mL is treated on cell culture. Posterior to DEP exposure, cells were incubated for 2 more days until immunofluorescence staining. The procedure for immunofluorescence staining is described above. As an epithelial marker and a mesenchymal marker, the expression of E-cadherin and alpha-SMA were observed.

TGF-beta is a multifunctional cytokine that prevents the proliferation of most types of cells, including epithelial cells and endothelial cells [47]. Numerous studies have revealed that TGF-beta stimulates epithelial-to-mesenchymal transition (EMT) in certain epithelial cells [47]. In this experiment, knowing that TGF-beta is a strong inducer of EMT, it is used to estimate the strength of DEP as an EMT inducer.

2.7 Asthma Mouse Model Preparation

Animals were bred and maintained in the AAALAC-International-accredited facility (#001169) and all animal experiments were approved by the Institutional Animal Care and Use Committee in Seoul National University Hospital (SNUH-IACUC). Animal study was prepared and performed by laboratory of mucosal immunity in Department of Biomedical Sciences, Seoul National University. Preparation of asthma mouse model is briefly introduced in Figure 2.9. A healthy mouse was exposed to papain, a known asthma inducing allergen, for three days and the mouse was allowed to rest for a week. A week after, 150 μg of DEP per one day was injected to the mouse using intra-nasal challenge for three days. On the day after last DEP injection, the mouse was sacrificed and its lung cells were tested for real-time PCR. For statistical analysis, the results from each of two groups, DEP and control, were compared with the Mann-Whitney U test. Difference between two groups is analyzed using SPSS (IBM, USA).

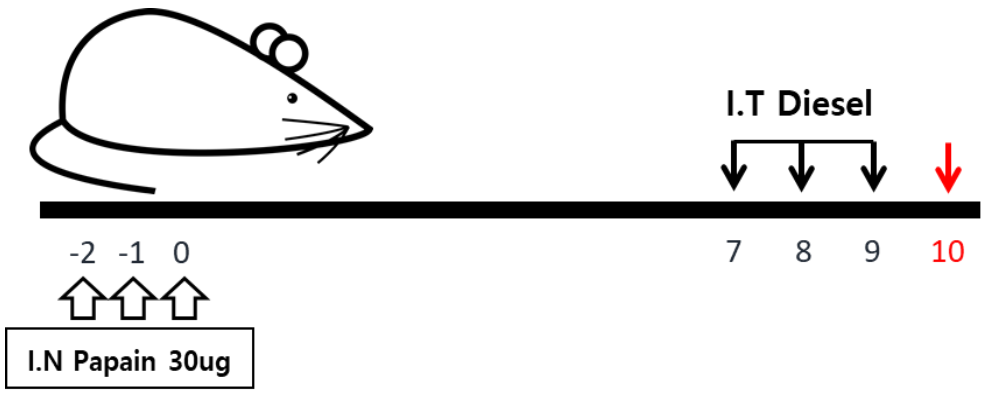

Group	Sensitization	7 ~ 9
Control	30μg Papain	6% DMSO
DEP	30μg Papain	150μg DEP

Figure 2.9 Schematic of mouse asthma model study. A healthy mouse was treated with papain for three days to induce asthma. After resting for a week, a mouse in experimental group was exposed to DEP for three consecutive days, while a mouse in control group was exposed to DMSO. A mouse is sacrificed on the day after, indicated by red arrow.

Chapter 3. Results

3.1 Development of a microfluidic Airway Epithelium-on-a-Chip

The microfluidic Airway Epithelium-on-a-Chip is made of a clear, flexible PDMS polymer and composed of upper and lower microchannels separated by a porous fibronectin-coated PET membrane (Figure 3.1). There are two additional channels branching from the center of the upper channel, which enables in-series co-culture of two different airway epithelial cells. Figure 3.1 provides a simple diagram of the cells cultured on chip. Two different epithelium are indicated by different color blocks and the perfusion of media is described as transparent red block in lower channel, under the porous membrane, indicated by yellow block. In-series co-culture is also schematically illustrated by transverse sectional diagram in Figure 3.1. Co-culture of nasal epithelial cells and alveolar epithelial cells was achieved by the protocol introduced in Method section. As shown in Figure 3.2, each epithelial cell is seeded on each end of upper channel, forming interaction of two cells at the center.

In order to make sure that each epithelial cell is properly seeded in the desired region, microscopic images of different regions and the formation of tight junction are provided section below. Morphological characteristics of each epithelial cell are investigated in microscopic images and compared to those from literature.

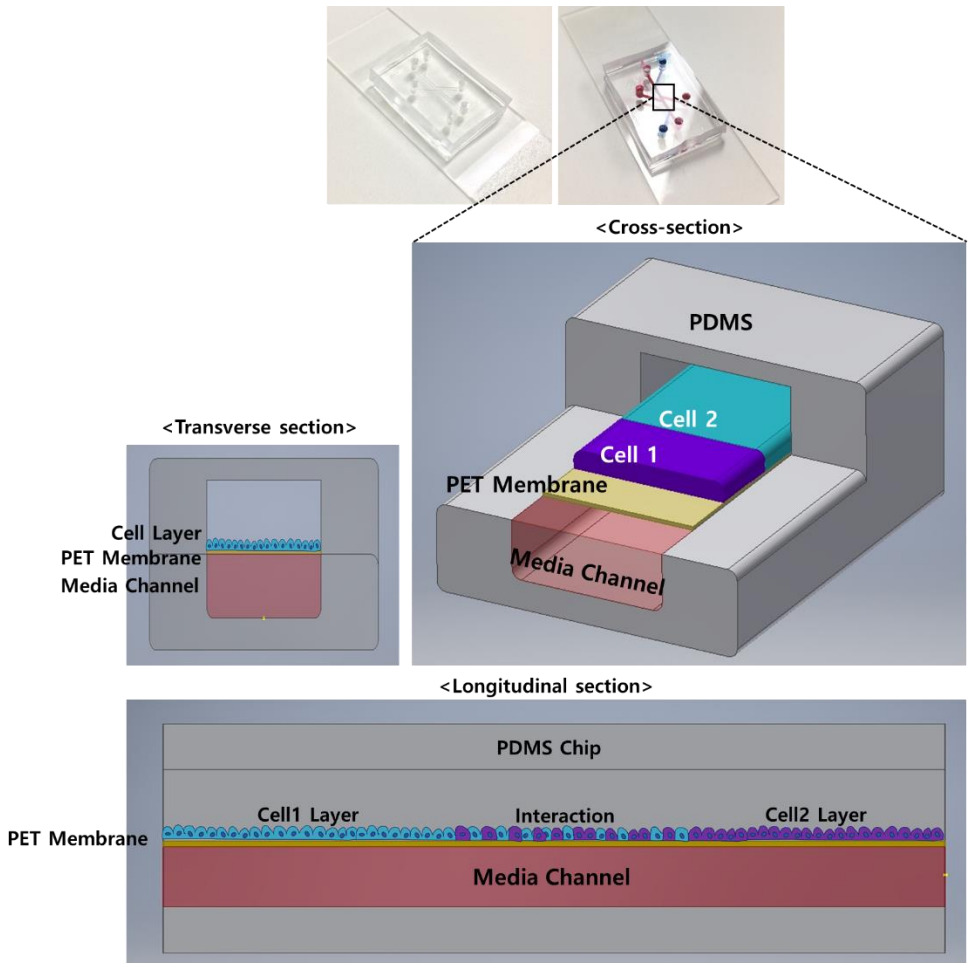

Figure 3.1 Image of an actual chip and its schematic diagrams. Cross section, transverse section and longitudinal section are provided for the concept of Airway Epithelium-on-a-Chip. Purple block indicates alveolar epithelial cell line (A549) and blue block indicates nasal cavity epithelial cell line (RPMI2650). A thin yellow sheet indicates the fibronectin-coated PET membrane, where cells are cultured. The perfusion of cell culture medium is described as transparent red block. The gray block indicate the entire device made of PDMS.

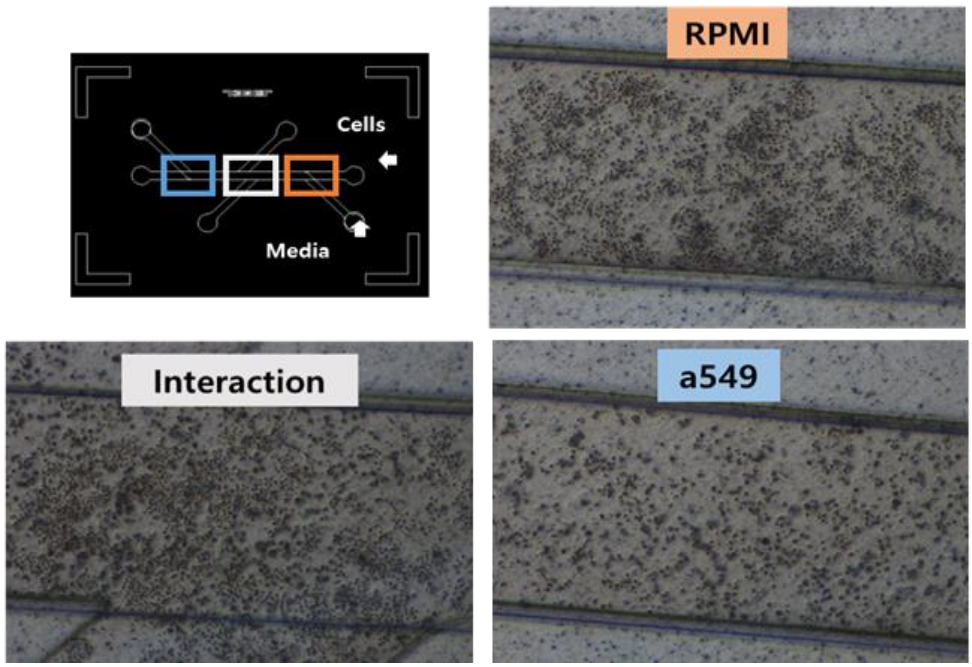

Figure 3.2 Microfluidic cell culture of two different airway epithelial cells. Nasal cavity epithelial cells and alveolar epithelial cells were cultured on each end of upper channel, making the interaction of two cells at the center of the channel. Microscopic images are taken on the day after cell culture.

When nasal cavity epithelial cell line (RPMI2650) and human alveolar epithelial cell line (A549) were cultured on the fibronectin-coated porous membrane in the top channel for 4 days under consistent perfusion of 50 μL/hr, mimicking fluid flow of the respiratory tract, the cultured epithelial cells continuously proliferated to form epithelium that exhibits tight junctions (Figure 3.3). The formation of tight junctions between epithelial cells could be observed by the expression of tight junction protein, E-cadherin. As shown in Figure 3.3, the expression of E-cadherin is seen with green in immunofluorescence stained image. Moreover, daily basis light-microscopic images of center region of the channel clearly show that the cultured epithelial cells proliferate until confluency for four days (Figure 3.4).

Not only the center region of the channel, but right and left sides of the channel were also imaged under light microscope. From day 1 to day 4, alveolar epithelial cells that are cultured on left side of the channel were proliferated until full confluency, and showed their morphological changes over time (Figure 3.5). Likewise, the proliferation of nasal cavity epithelial cells that are cultured on right side of the channel were observed with microscopic images (Figure 3.6).

A549 cells usually have a polygonal shape and sheet-like pattern in normal culture condition [48]. As they attach to surface, they tend to change their shape into long-spun cells, as if their vertexes of polygonal shape are drooped (Figure 3.7). On the other hand, nasal epithelial cells grow as they agglomerate together to form larger clusters [49]. Though they were dispersed over the channel on day 1, they had become crumpled into larger mass over time (Figure 3.8). These morphological features of each epithelial cell culture are observed in other researches [48-49]. Overall, the proliferation of cells on the entire channel is shown in Figure 3.9.

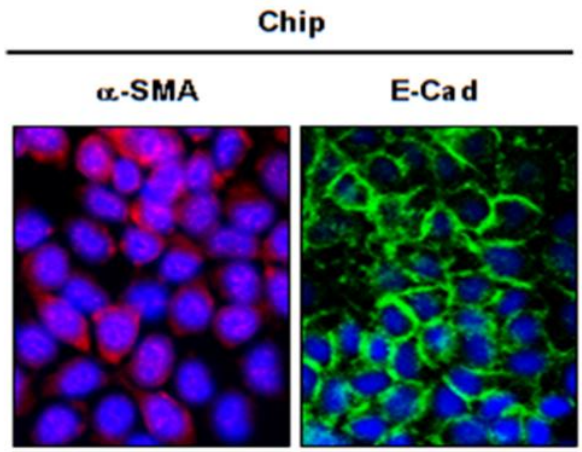

Figure 3.3 Expression of E-cad and alpha SMA from A549 cells cultured on a chip. The cell-seeded chip is incubated for two days and disassembled for immunofluorescence staining. E-cadherin (green), a known evidence for tight junction formation, is highly expressed.

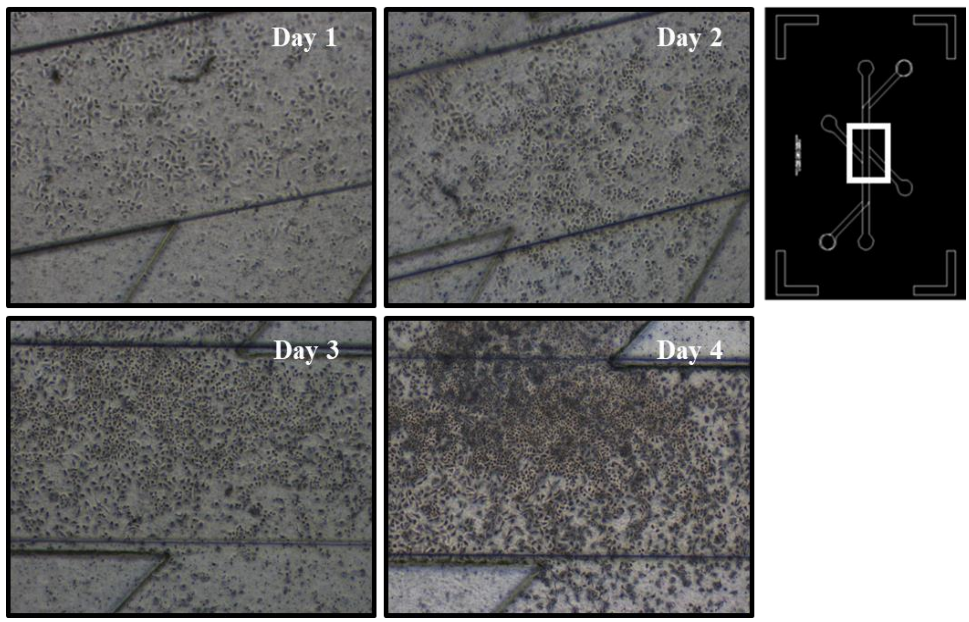

Figure 3.4 Daily based microscopic images of cells cultured on a chip. White box on the channel design (right) indicates the region of microscopic image. Confluency of two different epithelial cells inside the airway epithelium chip (A549 and RPMI 2650). Note that cell proliferates to fill the channel as day passes. About 100% confluency is achieved within three-four days.

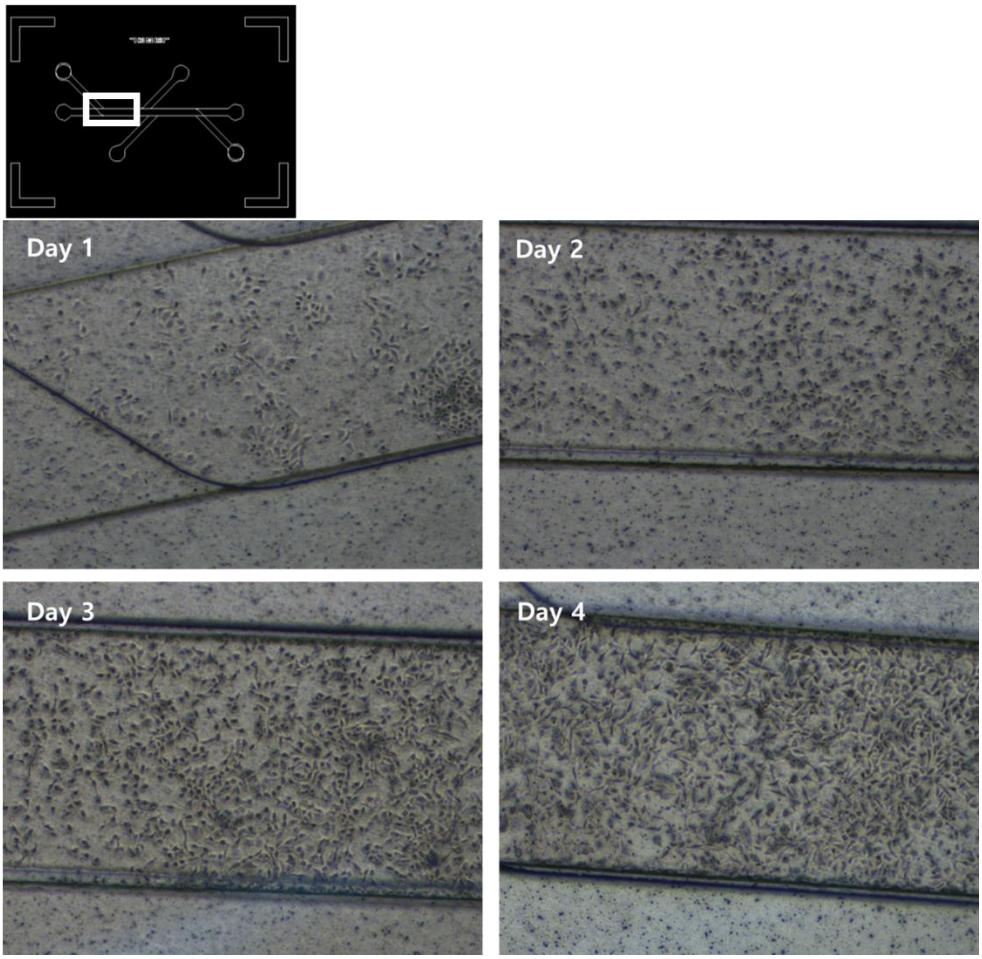

Figure 3.5 Daily based microscopic images of A549 cells cultured on chip. White box on the channel design (top) indicates the region of microscopic imaging. Confluency of human alveolar epithelial cells inside the airway epithelium chip is observed from the day after seeding (Day 1) to the day of DEP exposure (Day 4). The morphological characteristic of A549 cells, which is the elongated spindle shape, can be observed as day goes.

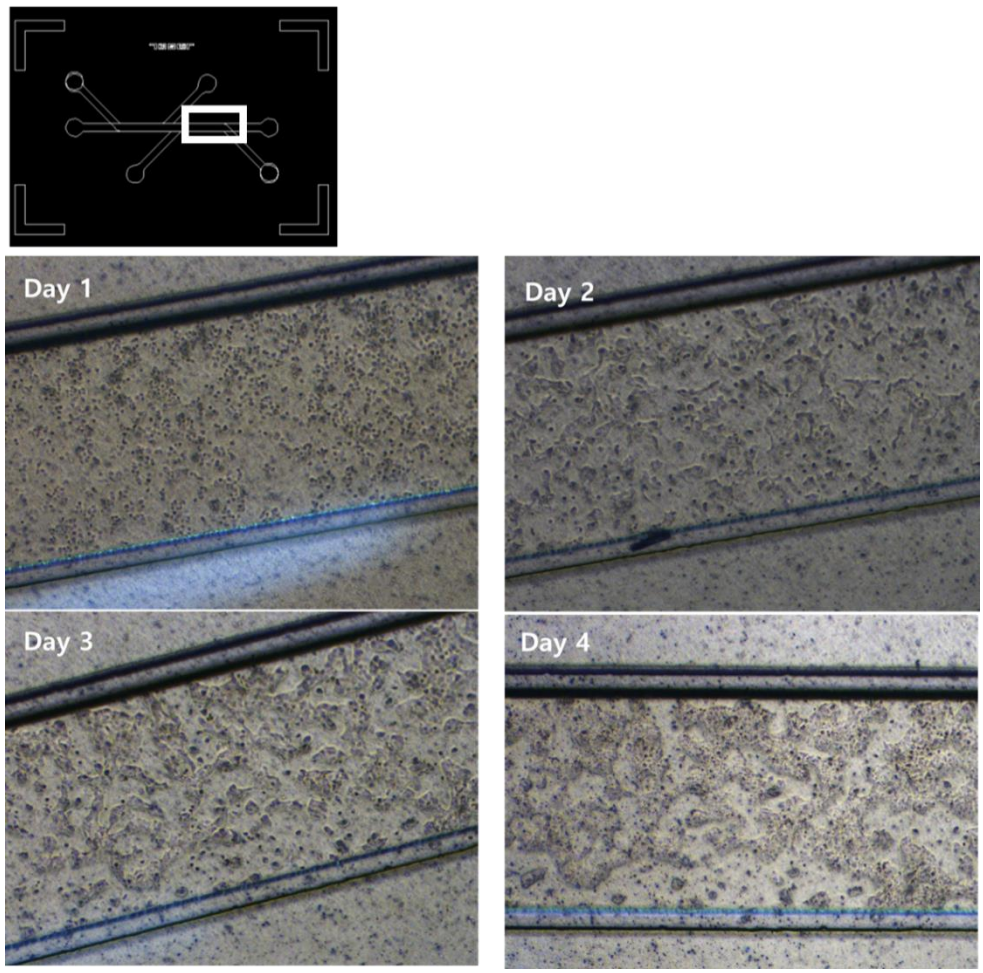

Figure 3.6 Daily based microscopic images of RPMI 2650 cells cultured on chip. White box on the channel design (top) indicates the region of microscopic imaging. Confluency of human nasal cavity epithelial cells inside the airway epithelium chip is observed from the day after seeding (Day 1) to the day of DEP exposure (Day 4). The characteristic of RPMI 2650 cell culture, which is the local accumulation of cells, can be observed as day goes.

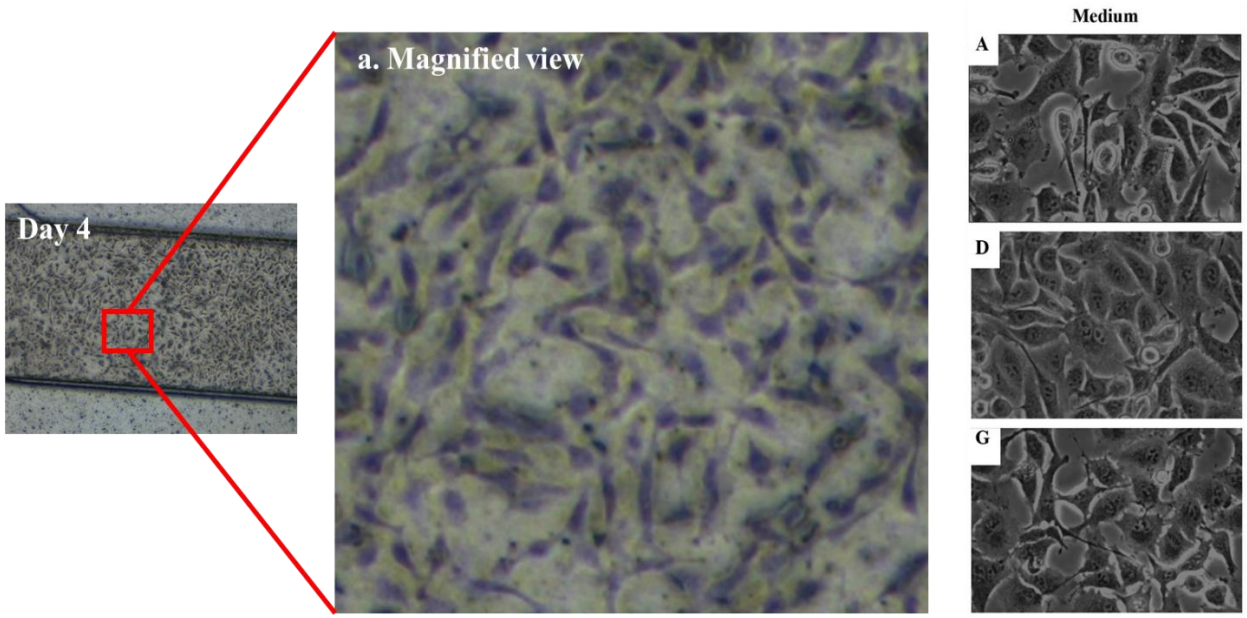

Figure 3.7 Magnified view of A549 cells cultured on chip and on literature. Red box indicates the magnified region of the channel. The cellular morphology of A549 cells can be observed, showing their polygonial shapes. On the right is the microscopic image of A549 from literature, showing similar morphological features as on-chip image. The microscopic image of A549 cells on the right is adapted from Soto-Nunez et al. [48].

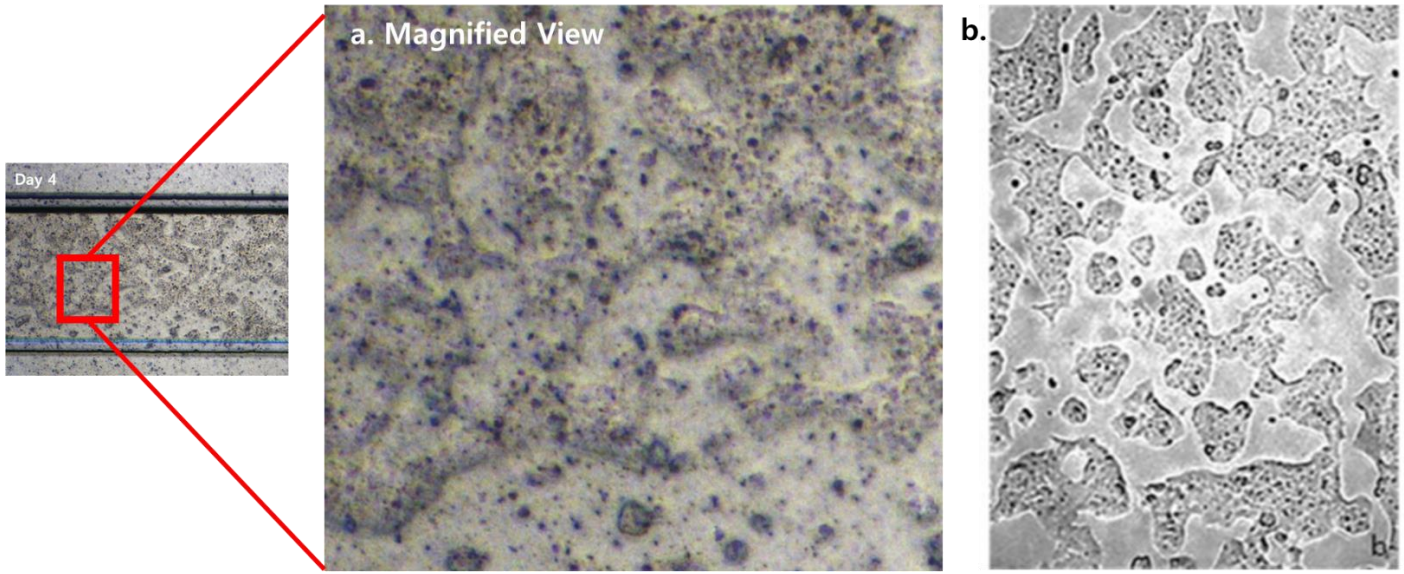

Figure 3.8 Magnified view of RPMI 2650 cells cultured on chip and on literature. Red box indicates the magnified region of the channel. The cellular morphology of RPMI 2650 cells can be observed, showing the formation of round-shaped agglomerate. The morphology of RPMI2650 cells on chip is same as that on literature, as shown in b. The microscopic image of RPMI 2650 cells on the right is adapted from Philicheva et al. [49].

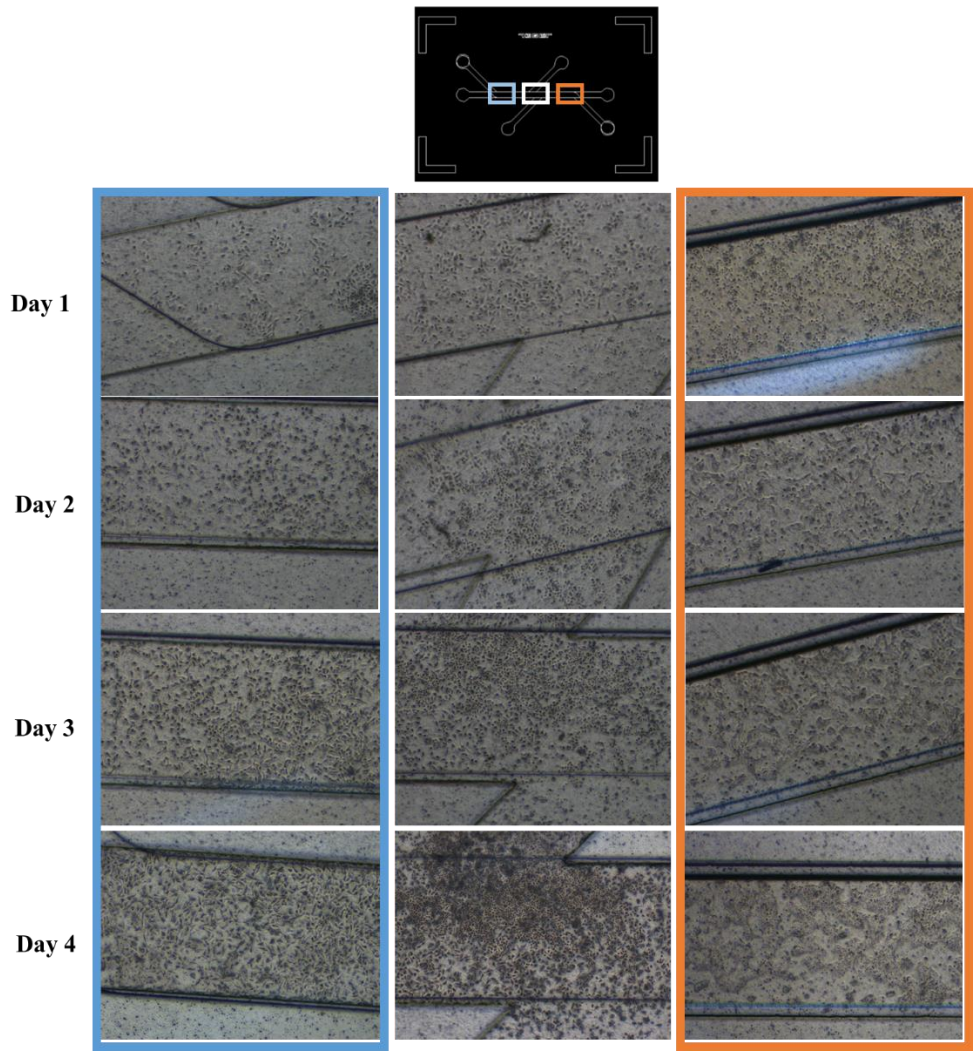

Figure 3.9 Daily based microscopic images of whole device. Both nasal and alveolar epithelial cells are cultured on chip and proliferated until full confluency during four days. Day 1 indicates the day after cell culture.

3.2 Microscopic Image Analysis

Microscopic images were analyzed to detect the degree of confluency, according to the algorithm mentioned above. The actual image processing procedure is shown in Figure 3.10. From the adjusted images, the region of interest, in this case, the central channel, was selected. Then the image was binarized to make any pixels whose threshold is under certain value be black. The image is transformed to logically-not and only the selected region is shown as a processed image. Microscopic images on each day of cell proliferation were processed and the results are shown in Figure 3.11. As shown, the region of cell layer is indicated by objects connected in white, and increased as the day passes from 1 to 4. On the day 4, most region of the central channel is covered with white. For quantitative measure, the pixel value for area in white is calculated and presented in Figure 3.11.

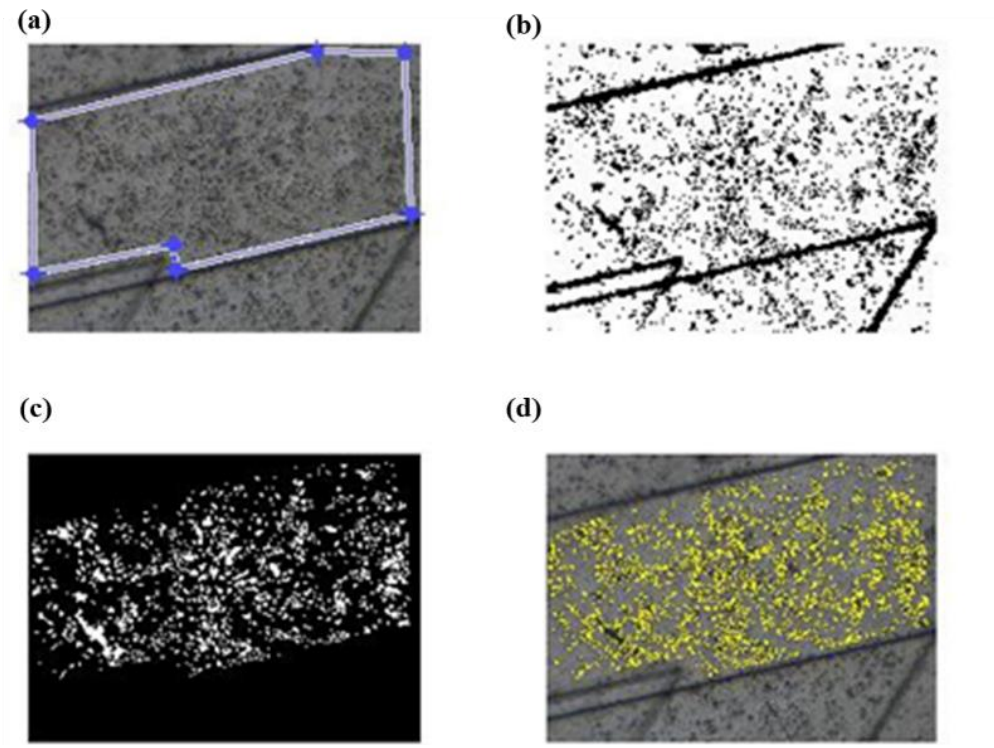

Figure 3.10 Image processing procedure. (a) The region of interest is selected by setting the points of polygon. (b) The image is binarized. (c) The image is transformed to logically not. (d) only the boundaries of image in (c) is overlapped with the original image

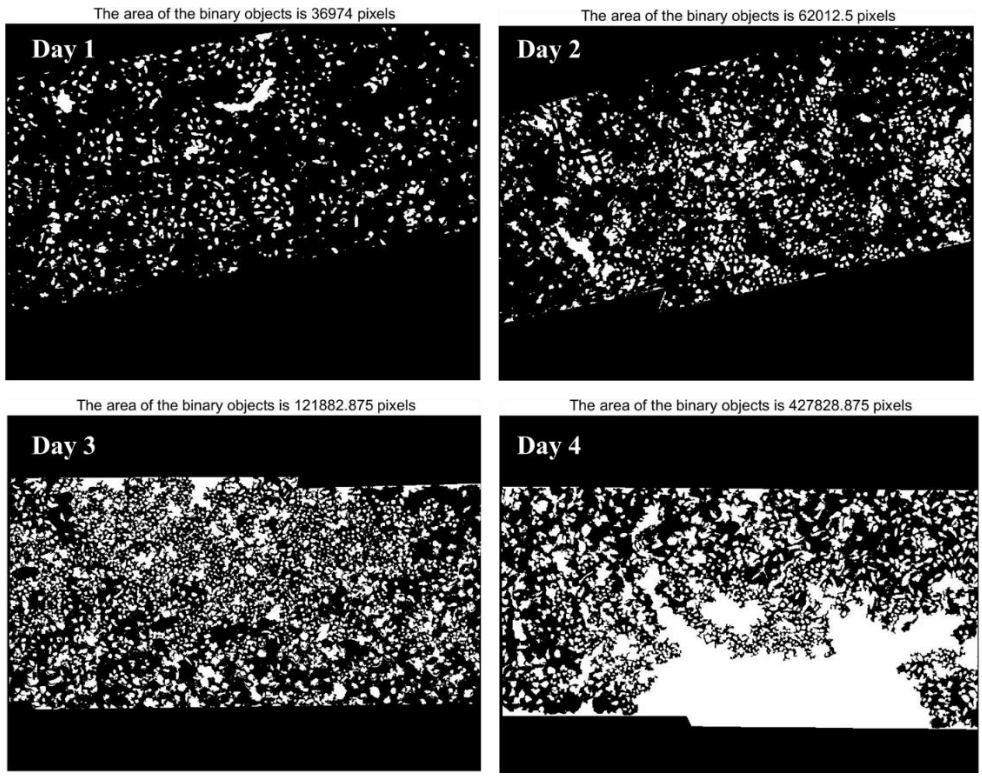

Figure 3.11 Image processing results. Images are processed according to the procedure described above, to show how cells proliferate as time goes. White blocks indicate cultured cells in microscopic image, which gradually increase from day 1 to day 4. On day 4, the region of interest is almost filled with white blocks, indicating the full confluency on the chip. The area of objects in white, which indicates cell-covered area, increases from day 1 to day 4, resulting in 427829 pixels on day 4.

3.3 Effects of DEP on Airway Epithelium-on-a-Chip

In order to test the functionality of our microfluidic device for assessing effects of any PM substances on airway epithelium, DEP, a known PM component, was used as a chemical stimulation agent. 50 μL of DEP (Concentration: 50 μg/mL) was flown into the upper channel via micropipette, directly stimulating airway epithelium formed inside the chip. To find out the effect of DEP on cells inside the chip, RNAs were extracted from the cells and underwent for PCR. The PCR results are shown in Figure 3.12, which clearly states the elevation of IL-6 and IL-8 cytokines. Since those chips that were not treated with DEP show clearly lower expression of these cytokines, it can be concluded that DEP caused the cells to express these inflammatory cytokines. Statistical analysis on this result could not be conducted for lack of experimental samples. During this research, only one experimental set, containing 4 microfluidic chips, had gone through DEP exposure. Moreover, 4 chips were divided into two groups, control and experimental groups and all cells in each group were collected together for PCR analysis. Therefore, no error bar is presented in Figure 3.12.

To find out other effects of DEP on airway epithelium, cells were tested to see if their EMT ability has been affected by DEP. After treated with DEP, epithelial cells inside the chip were sit inside the incubator for 48 hours, and then immunofluorescence-stained to discover the expression level of EMT markers. Non-DEP-treated chip was also stained as a control group of this experiment. As shown in Figure 3.13, the epithelial marker, E-cad, is clearly less expressed in DEP group than in a control group, whereas alpha-SMA, the mesenchymal marker, is clearly more expressed in DEP group than in a control group. This result suggest that DEP triggers epithelial cells to fall apart, breaking tight junctions between cells.

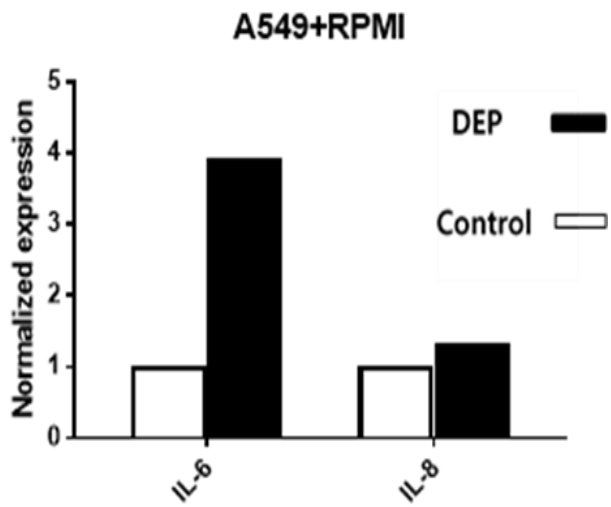

Figure 3.12: Expression of pro-inflammatory cytokines (IL-6 and IL-8) as a result of DEP exposure on Airway Epithelium-on-a-Chip. White blocks indicate the control group, on which DEP is not treated, while black blocks indicate DEP group. Significant increase of IL-6 expression is observed, while comparably little elevation of IL-8 is observed. (n=1 for DEP and control group)

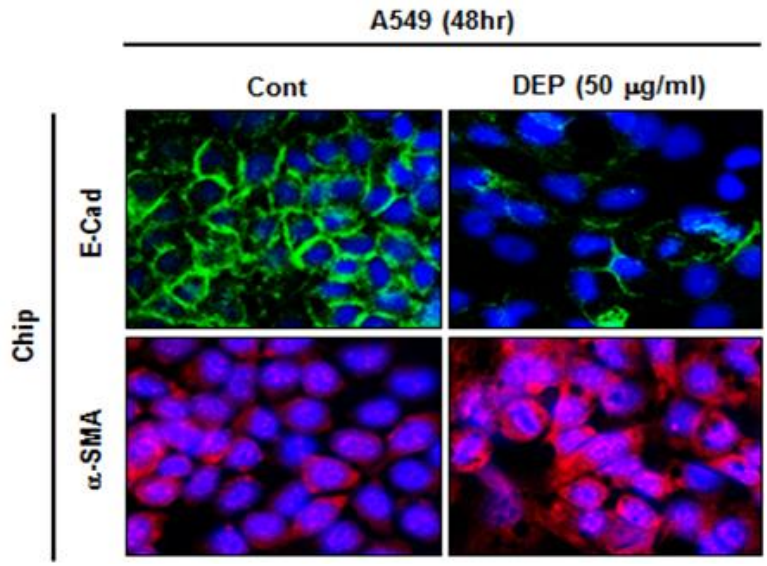

Figure 3.13 Expression of EMT markers in A549 cell line on a chip. E-cadherin, an epithelial marker, is less expressed on DEP-treated chip, while alpha-SMA, a mesenchymal marker, is more expressed.

3.4 Effect of DEP on *in-vitro* and Asthma Mouse Model Study

In order to establish the reliability of Airway Epithelium-on-a-Chip, both in-vitro and in-vivo experiments on DEP were held and the corresponding results were compared with those from the microfluidic chip. In-vitro experiment was used to verify the effect of DEP on EMT ability of epithelial cells. cells were cultured on a cell-culture plate and treated with DEP. 48 hours later, DEP treated cells were stained to see the expression of EMT markers. As shown in Figure 3.14, DEP made the expression of E-cad, the epithelial marker, decreased. Compared to the image of the control group, the images of DEP group show less E-cad expressed (green). Cells treated by TGF-beta, not by DEP, showed the least expression of E-cad. On the other hand, the expression of alpha-SMA, the mesenchymal marker, was clearly increased in DEP groups, compared to the control group (red). TGF-beta group shows the most expression of alpha-SMA.

In-vivo experiment was used to verify the inflammatory reaction of airway epithelium, which was caused by DEP exposure. Asthma-induced mouse was treated with 150 μg of DEP for three days and its lung cells were undergone through real-time PCR. This in-vivo experiment was performed to check if the results from the chip are same as those from the animal study. Though not presented as graphs or figures, many inflammatory cells around airway were found to crowd in its lung tissue. This results draw a conclusion that DEP, an air pollutant, can aggravate the inflammation inside respiratory tract. Moreover, as an asthma-induced mouse was exposed to DEP, airway epithelium was found to secrete inflammatory cytokines that call for immune cells to gather. As one such cytokine, the mRNA level of IL-6 cytokine was higher in DEP-treated mouse that in control mouse (Figure 3.15). Statistical analysis using SPSS also showed the p value of the Mann-Whitney U test is less than 0.05, which states that IL-6 level of DEP group is statistically significantly higher than that of control group.

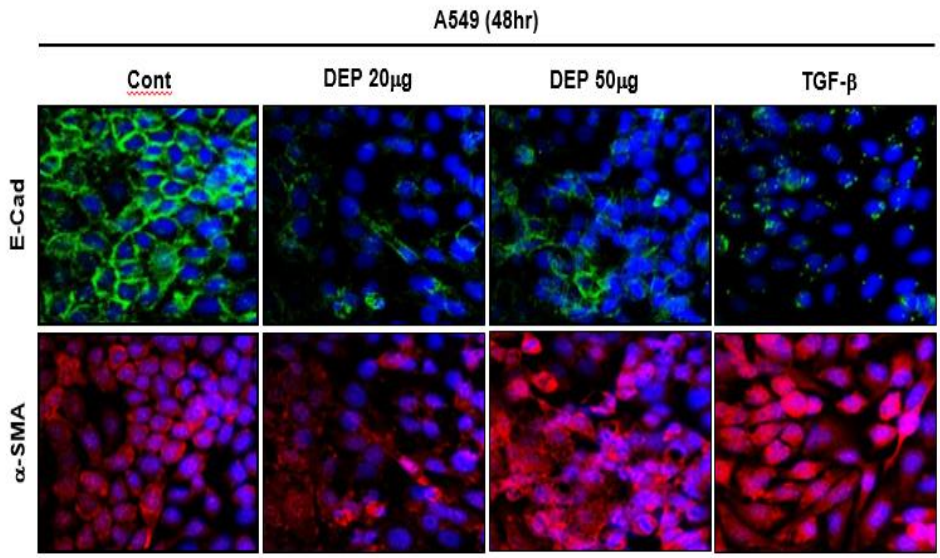

Figure 3.14 Expression of EMT markers in A549 cells cultured on plate. Cultured cells were observed under microscopy to see the epithelial formation. Control group has no DEP exposure and DEP group has two different concentrations of DEP. High expression of E-cadherin in control group verifies the formation of epithelium. TGF-beta is treated as a strong EMT inducer. E-cadherin (green), epithelial marker, is notably less expressed on DEP-treated group, while alpha-SMA (red), mesenchymal marker, is more expressed on DEP treated group. The expression of alpha-SMA is highest in TGF-beta group, showing DEP is less powerful than TGF-beta as an EMT inducer.

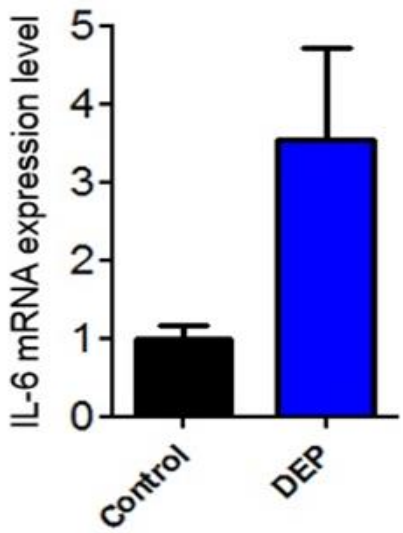

Figure 3.15 Elevation of IL-6 mRNA expression in the mouse asthma model. Asthma-induced mice were exposed to DEP for three days. On the fourth day, the mouse is sacrificed and its lung cells are undergone for PCR. PCR result indicates higher expression of IL-6 mRNA level in DEP group, which becomes pro-inflammatory cytokines. IL-6, a known inflammatory cytokine, is known for recruiting immune cells and leading to initial stage of inflammation. ($p < 0.05$ for Mann-Whitney U test, analyzed by SPSS)

Chapter 4. Discussion

4.1 Airway Epithelium-on-a-Chip as a Novel 3D *in-vitro* Model

Airway Epithelium-on-a-Chip was designed to develop a novel *in-vitro* model of human airway epithelium. To mimic 3D structure of human airway epithelium, in-series co-culture technique, perfusion-based long-term cell culture system and ECM-coated membrane were collaborated. Using the novel microfluidic cell culture technique, the formation of two epithelium inside the chip was made. Both nasal and alveolar epithelial cells cultured on different sides of the channel showed their own morphological features on the channel and had their interaction on the center of the channel. As they proliferated on the channel, their morphological features had become more vivid, and thus proving capability of the design of the microfluidic channel.

The proliferation of alveolar epithelial cells and nasal epithelial cells was observed inside the chip. Also, the expression of E-cad from the on-chip cultured cells shows the formation of tight junctions, which means the continuous cell-to-cell barrier between epithelial cells. This barrier between cells separates tissue space and regulates intercellular movements of molecules, which explicates the formation of epithelium on the chip [50]. In contrast, the lack of alpha-SMA expression shows no vivid EMT ability measured, which also tells continuous proliferation of epithelial cells on the chip [51]. Image-processed microscopic images also verify that cells proliferate to form epithelial layer within 4 days. Formation of such epithelial layer on chip shows that in-series co-culture of RPMI2650 and A549 is possible using a novel

microfluidic cell culture technique.

To explore the potential of the microfluidic device in assessing PM effects on airway epithelium, Airway Epithelium-on-a-Chip was treated with a certain amount of DEP. As a consequence, tight junctions of on-chip cultured cells were broken and the level of inflammatory cytokines, IL-6 and IL-8, was elevated. Similar results could be found in simultaneously held in-vitro and in-vivo studies. On the in-vitro experiment, where cultured human alveolar epithelium was treated with DEP, the breakage of tight junctions was observed as an effect of DEP. The reason for such breakage is considered as EMT, which transforms tightly connected epithelial cells into mesenchymal cells. The EMT ability of DEP could be evaluated as compared to that of TGF-beta. Showing less expression of alpha SMA than cells treated by TGF-beta, the EMT ability of DEP is thought to be less than that of TGF-beta. On the in-vivo experiment, an asthma-induced mouse was treated with DEP, showing increased IL-6 mRNA level. By showing that the on-chip results are same as those performed in-vivo and in-vitro, the functionality and the reliability of Airway Epithelium-on-a-Chip were assured.

As a 3D in-vitro model, Airway Epithelium-on-a-Chip implies few significant points. First, the ability to culture two different epithelial cells in one channel signifies a potential to analyze the interaction between different epitheliums. Not only airway epitheliums, any consecutively lined epitheliums can also be reconstituted as an in-vitro model, using this design. Also, more than two different epithelial cells can be cultured if more branches along the center channel are added.

The second point is its effectiveness as an in-vitro model. With the soft-lithographed silicon mold, the device can be made repeatedly, without quality loss. This makes it far cheaper than any in-vivo models, and even competent to win in-vitro models, considering long-term costs. Composed of PDMS and PET membrane, the microfluidic device provides more physiological similarity than any in-vitro models. The continuous perfusion system by a syringe pump mimics human vascular perfusion and the fibronectin-coated membrane imitates the

extra-cellular matrix under epithelium. These features make our device a strong 3D in-vitro model. The effectiveness of our device can be more supported by the efficient experiment environment that the microfluidic chip brings. The presence of microchannel enables easy-loading and use of comparably small amounts of chemicals in interests, which keeps experiments from waste of time and materials.

4.2 On-chip Inflammatory Reaction to DEP

The most important aim of this research is to develop the Airway Epithelium-on-a-Chip as a platform for assessing the effects of PM on airway epithelium. To do that, our chip needs to have the ability to investigate how PM affects airway epithelium, which, in most cases, is inflammation. In this research, the expression of inflammatory cytokines is focused as the evidence of inflammation, because the airway epithelial cells are responsible for the synthesis and release of cytokines in sites of inflammation [52]. As a consequence, the released inflammatory cytokines recruit, retain, and accumulate various inflammatory cells [53].

The on-chip results shows the increase of IL-6 and IL-8, which are known pro-inflammatory cytokines. The elevated expression of IL-6 and IL-8 in airway epithelium creates chemotactic gradient and induces transepithelial neutrophil migration. The underlying mechanism for inflammatory cell migration is still unclear, but the involvement of p38 MAPK activity in the production and regulation of IL-6 and IL-8 has been reported [52, 54-55]. Generally, IL-6, when synthesized during the initial stage of inflammation, moves to the liver through the bloodstream, which causes rapid induction of sequential stages of inflammation [56]. It also promotes specific differentiation of T cells, thus performing an important function in connecting inflammation to immune response [57]. IL-8, another cytokine of our interest, is also responsible for the recruitment of neutrophils and macrophages into the site of

inflammation.

The increase of IL-6 and IL-8 expression as a result of airway epithelial damage can be found in many other studies. The release of cytokines from lung surface epithelium was shown in the study of Sun et al., where A549 was used as lung epithelial cells [58]. The study of Chow et al. shows that damage to the bronchial epithelia by poly-L-arginine stimulates polarized IL-6 and IL-8 secretion. In that study, human bronchial epithelial cells were chemically injured by the foreign material resulting in elevated IL-6 and IL-8 mRNA expressions [59]. This result is significantly similar to the result from our research, adding credits to ours.

The effects of DEP on airway epithelium were also investigated in many in-vitro studies [27-30, 33, 60]. In the study of Sydbom, human alveolar epithelial cells engulfed DEP and released pro-inflammatory cytokines like IL-6 and IL-8 [60]. The study of Tomasket et al. investigated the combinational effect of DEP and volcanic ash, which also resulted in significant increase of pro-inflammatory cytokines, including IL-8 [61]. These results are clearly similar to the on-chip results, assuring the functionality of Airway Epithelium-on-a-Chip.

The result from the asthma mouse model also shows that the level of IL-6 mRNA from mouse lung cells is increased as an effect of DEP, which corroborates the on-chip result. By showing that the on-chip result is significantly similar to those from other literatures and the simultaneously conducted animal study, the potential of Airway Epithelium-on-a-Chip to be a platform for investigating PM effect on airway epithelium has been demonstrated.

4.3 Limitations & Future Works

Airway Epithelium-on-a-Chip, despite its promising results shown in this research, has many limitations that need further works. One limitation of the chip is the absence of endothelial lining on the other side of PET membrane. Human tissue consists of epithelium, ECM, and endothelium or blood vessels. To mimic this structure, many organ-on-chips are constructed with epithelial cells of interest, ECM material of choice, and primary endothelial cells [39-46]. Co-culture of epithelial and endothelial cells on each channel of a chip enables the investigation of the molecular transport between two cells [41]. However, as our device did not have endothelial cells lined on the chip, more advanced reconstruction of airway tissue was not made.

Another limitation is that our microfluidic device did not show formation of mucins and cilia from airway epithelial cells. Formation of cilia and secretion of mucins are primary signs of airway epithelial differentiation [39] for they act as filters and surfactants to keep the epithelial surface clean and mucous [26]. However, we did not have chances to see those signs of differentiation in our chip. Main reason lies on the use of cell lines rather than primary cells, where the rate of proliferation and differentiation varies significantly. Using cell lines of interest, our chip was confluence within 3 to 4 days, and then the rate of proliferation diminished, showing unhealthy state of cells. For this reason, DEP experiments were performed right after achieving cell confluency in the chip.

Other technical challenges of general Organ-on-Chips should be concerned. Bubbles in microfluidic channels can damage cells, while they are hard to remove. Moreover, continuous perfusion can be harmful since chances of contamination are higher than conventional cell culture methods. Additional challenges include achieving stable reproducibility of microfluidic cell-culture, where it highly depends on works of skilled person.

In order to overcome such limitations, use of primary nasal epithelial and alveolar epithelial

cells is inevitable. Since primary cells are originated from real human tissues, they would provide the exact physiology of airway epithelial cells as they do in human body. Use of primary cells will also enable more advanced differentiation of cells, which results in fully developed cilia and secretion of mucin on apical surface of epithelium. Moreover, as primary cells show normal proliferation rate, which is much slower than that of cell line, much longer cell culture periods can be made inside the chip. This would provide more stable epithelium, also stabilizing experimental results. Also, endothelial cell culture inside the chip should be performed for reconstituting organ-level functions of airway epithelium. Development of air-liquid interface on the airway epithelium surface should be studied for differentiation of cells, for airway epithelial cells meet air flow when residing in human body. When these further plans are made and Airway Epithelium-on-a-Chip is advanced, different PM candidates other than DEP should be tested for their inflammatory reactions.

Chapter 5. Conclusion

In this research, Airway Epithelium-on-a-Chip is developed and used for investigating its reaction to DEP. PDMS-based microfluidic chip, fabricated using soft-lithography method, is consisted of in-series co-culture upper layer, fibronectin-coated membrane and lower channel with continuous perfusion of media. Using the novel microfluidic cell-culture technique, nasal and alveolar epithelial cells were successfully cultured on upper channel, which mimics the consecutive epithelial lining of the respiratory tract. Consequently, the proliferation of nasal and alveolar epithelial cells was observed throughout the entire upper channel. Although nasal epithelium is not connected to alveolar epithelium in actual human respiratory tract, this novel in-series co-culture of two different cells provides potential to recapitulate any consecutive epithelium on a microfluidic channel.

Experimental results of this research reflect successful development of Airway Epithelium-on-a-Chip and its functionality for PM study. Simultaneous in-vitro and animal study also reflect the reliability of the on-chip results. As an important finding, epithelial cells cultured inside the chip expressed increased levels of IL-6 and IL-8, which are known inflammatory cytokines, and many academic studies have demonstrated same results as ours.

To conclude, this research achieved the development of Airway Epithelium-on-a-Chip and discusses its potential as a platform for studying PM effects on airway epithelium.

References

1. S. Buchholz, J. Junk, and A. Krein, et al., "Air pollution characteristics associated with mesoscale atmospheric patterns in northwest continental Europe," *Atmospheric Environment*, vol. 44, pp. 5183–5190, 2010.

2. U.S. EPA (United States Environmental Protection Agency), "The particle pollution report: Current understanding of air quality and emissions through 2003," *EPA*, Research Triangle Park, NC, 2004.

3. B. Brunekreef, and ST. Holgate, "Air pollution and health," *Lancet*, vol. 360, pp. 1233–1242, 2002.

4. M. Kampa, and E. Castanas, "Human health effects of air pollution," *Environ Pollut*, vol. 151, pp. 362–367, 2008.

5. B. Bowe, Y. Xie, and T. Li, et al., "Particulate Matter Air Pollution and the Risk of Incident CKD and Progression to ESRD," *J. Am. Soc. Nephrol*, vol. 28, 2017

6. S. H. Hwang, J. Y. Lee, and S. M. Yi, et al., "Associations of particulate matter and its components with emergency room visits for cardiovascular and respiratory diseases," *PLoS ONE12*, vol. 8: e0183224, 2017.

7. R. D. Brook, B. Franklin, and W. Cascio, et al., "Air pollution and cardiovascular disease: a statement for healthcare professionals from the Expert Panel on Population and Prevention," *Science of the American Heart Association. Circulation*, vol. 109, pp. 2655–2671, 2004

8. L. Calderon-Garciduenas, B. Azzarelli, and H. Acune, et al., "Air pollution and brain damage," *Toxicol Pathol*, vol. 30(3), pp. 373-389, 2002.

9. H. Lin, J. Tao, Y. Du, and T. Liu, et al., "Differentiating the effects of characteristics of PM pollution on mortality from ischemic and hemorrhagic strokes," *Int J Hyg Environ Health*, vol. 219, pp. 204-211, 2016.

10. C. M. Wong, N. Vichit-Vadakan, and H. Kan, et al., "Public Health and Air Pollution in Asia (PAPA): a multicity study of short-term effects of air pollution on mortality," *Environ Health Perspect*, vol. 116, pp. 1195, 2008.

11. A. J. Cohen, and M. Ezzati, "Global and regional burden of disease attributable to selected major factors," Geneva, World Health Organization, vol. 2(17), pp. 1354-1433, 2004.

12. S. S. Lim, T. Vos, and A. D. Flaxman, et al., "A comparative risk assessment of burden of disease and injury attributable to 67 risk factors and risk factor clusters in 21 regions, 1990–2010: a systematic analysis for the Global Burden of Disease Study 2010," *Lancet*, vol. 380, pp. 2224-2260, 2012.

13. S. Buchholz, J. Junk, and A. Krein, et al., "Air pollution characteristics associated with mesoscale atmospheric patterns in northwest continental Europe," *Atmos Environ*, vol. 44, pp. 5183-5190, 2010.

14. J. K. Zhang, Y. Sun, and Z. R. Liu, et al., "Characterization of submicron aerosols during a month of serious pollution in Beijing, 2013," *Atmospheric Chemistry, Phys*, vol. 14, pp. 2887-2903, 2014.

15. R. J. Park and S.-W. Kim, "Air quality modeling in East Asia: present issues and future

directions," *Asia-Pacific J. Atmos. Sci*, vol. 50, pp. 105-120, 2014.

16. D. G. Lee, Y. M. Lee, and K. W. Jang, et al., "Korean National Emissions Inventory System and 2007 Air Pollutant Emissions," *Asian J. Atmos. Environ*, vol. 5, pp. 278-291, 2011.
17. A.P. Sharma, K.H. Kim, and J.W. Ahn, et al., "Ambient particulate matter (PM10) concentrations in major urban areas of Korea during 1996–2010," *Atmos. Pollut Res.*, vol. 5, pp. 161-169, 2014.
18. K. Vellingiri, K. H. Kim, and C. J. Ma, et al., Brown, "Ambient particulate matter in a central urban area of Seoul, Korea," *Chemosphere*, vol. 119, 2015.
19. I. N. Krivoshto, J. R. Richards, and T. E. Albertson, et al., "The toxicity of diesel exhaust: implications for primary care," *J Am Board Fam Med*, vol. 21, pp. 55-62, 2008.
20. W. Majewski, Addy and K. Khai Magdi, "Diesel Emissions and Their Control," *SAE International*, pp. 584, 2006.
21. M. E. Parent, M. C. Rousseau, and P. Boffetta, et al., "Exposure to diesel and gasoline engine emissions and the risk of lung cancer," *American Journal of Epidemiology*, vol. 165, 2006.
22. A. Peretz, J. Kaufman, and C. Trenga, et al., "Effects of diesel exhaust inhalation on heart rate variability in human volunteers," *Environmental Research*, vol. 107, pp. 178–184, 2008.
23. J. Pourazar, I. S. Mudway, and J. M. Samet, et al., "Diesel exhaust activates redox-sensitive transcription factors and kinases in human airways," *Am J Physiol Lung Cell Mol Physiol*, vol. 289, pp. 724 –730, 2005.

24. M. Riedl and D. Diaz-Sanchez, "Biology of diesel exhaust effects on respiratory function," *J Allergy Clin Immunol*, vol. 115, pp. 221–228, 2005.

25. A. Don Porto Carero, P. H. Hoet, and L. Verschaeve, et al., "Geno-toxic effects of carbon black particles, diesel exhaust particles, and urban air particulates and their extracts on a human alveolar epithelial cell line (A549) and a human monocytic cell line (THP-1)," *Environ Mol Mutagen*, vol. 37(2), pp. 155-163, 2001.

26. R. Wilson, "Disposition of Particulate Matter (PM) in the Respiratory system," *Harvard Press*, 1996.

27. T. Ohtoshi, H. Takizawa, and H. Okazaki, et al, "Diesel exhaust particles stimulate human airway epithelial cells to produce cytokines relevant to airway inflammation *in vitro*," *J Allergy Clin lmmunol*, vol. 101, pp. 778-785, 1998.

28. H. Takano, T. Yoshikawa, and T. Ichinose, et al., "Diesel exhaust particles enhance antigen-induced airway inflammation and local cytokine expression in mice," *Am. J. Respir. Crit. Care Med*, vol. 156, pp. 36–42, 1997.

29. I. S. Mudway, N. Stenfors, and S. T. Duggan, et al., "An *in vitro* and *in vivo* investigation of the effects of diesel exhaust on human airway lining fluid antioxidants," *Arch Biochem Biophys*, vol. 423, pp. 200–212, 2004.

30. A. J. Ghio, C. B. Smith, and M. C. Madden, "Diesel exhaust particles and airway inflammation," *Current Opinion Pulm. Med.*, vol. 18, pp. 144-150, 2012.

31. D. Diaz-Sanchez, M. Jyrala, and D. Ng, et al., "*In vivo* nasal challenge with diesel exhaust particles enhances expression of the CC chemokines rantes MIP-1alpha, and MCP-3 in

humans," *Clin Immunol*, vol. 97, pp. 140–145, 2000.

32. R.B. Hetland, M. Refsnes, and T. Myran, et al., "Mineral and/or metal content as critical determinants of particle-induced release of IL-6 and IL-8 from A549 cells," *J Toxicol Environ Health*, vol. 60, pp. 47-65, 2000.

33. T. Ohtoshi, H. Takizawa, and H. Okazaki, et al., "Diesel exhaust particles stimulate human airway epithelial cells to produce cytokines relevant to airway inflammation *in vitro*," *J Allergy Clin lmmunol*, vol. 101, pp. 778-785, 1998.

34. D. Huh, G. A. Hamilton, and D. E. Ingber, "From 3D cell culture to organs-on-chips," *Trends in cell biology*, vol. 21, pp. 745-754, 2011.

35. S. G. Klein, J. Hennen, and T. Serchi, et al., "Potential of coculture *in vitro* models to study inflammatory and sensitizing effects of particles on the lung," *Toxicology. In Vitro*, vol. 25, pp. 1516-1534, 2011.

36. G. Bardet, V. Mignon, and I. Momasa, et al., "Human Reconstituted Nasal Epithelium, a promising *in vitro* model to assess impacts of environmental complex mixtures," *Toxicology. In Vitro*, vol. 32, pp. 55-62, 2016

37. S. G. Klein, T. Serchi, and L. Hoffmann, et al., "An improved 3D tetraculture system mimicking the cellular organization at the alveolar barrier to study the potential toxic effects of particles on the lung. *Part. Fibre Toxicology*, Vol. 10, 2013.

38. Y. Xia and G. M. Whitesides, "Soft lithography," *Annual review of materials science*, vol. 28, pp. 153-184, 1998.

39. D. Huh, B. D. Mathhews, and A. Mammoto, et al., "Reconstituting organ-level lung functions on a chip," *Science*, vol. 328, pp.1662-1668, Jun 25 2010.

40. H. J. Kim, D. Huh, and G. Hamilton, et al., "Human gut-on-a-chip inhabited by microbial flora that experiences intestinal peristalsis-like motions and flow," *Lab on a Chip*, vol. 12, pp. 2165-2174, 2012.

41. J. S. Lee, R. Romero, and Y. M. Han, et al., "Placenta-on-a-chip: a novel platform to study the biology of the human placenta," The Journal of Maternal-Fetal & Neonatal Medicine, vol. 29, pp. 1046-1054, 2016.

42. K. J. Jang, A. P. Mehr, and G. A. Hamilton, et al., "Human kidney proximal tubule-on-a-chip for drug transport and nephrotoxicity assessment," Integr. Biol., vol. 5, pp. 1119-1129, 2013.

43. L. M. Griep, F. Wolbers, and B. de Wagenaar, et al., "BBB on chip: microfluidic platform to mechanically and biochemically modulate blood-brain barrier function," Biomed Microdevice, vol. 15, pp 145-150, 2013.

44. D. Y. No, K. H. Lee, and J. Lee, et al., "3D liver models on a microplatform: well-defined culture, engineering of liver tissue and liver-on-a-chip," *Lab on a chip*, vol. 15, pp. 3822-3837, 2015.

45. B. Zhang, M. Montgomery, and M. Dean Chamberlain, et al., "Biodegradable scaffold with built-in vasculature for organ-on-a-chip engineering and direct surgical anastomosis," *Nature Materials*, vol. 15, pp. 669-678, 2016.

46. Y. S. Zhang, J. Aleman, and A. Arneri, et al., "From cardiac tissue engineering to heart-on-

a-chip: Beating challenges," *Biomed Mater*, vol. 10, 2015.

47. K. Miyazona, "Transforming growth factor-beta signaling in epithelial-mesenchymal transition and progression of cancer," *Proc Jpn Acad Ser B Phys Biol Sci.*, vol. 85, pp. 314-323, 2009.

48. M. Soto-Nunez, K. A. Diaz-Morales, and P. Cautle-Rodriguez, et al., "Single-cell microinjection assay indicates that 7-hydroxycoumarin induces rapid activation of caspase-3 in A549 cells," *Experimental and Therapeutic Medicine*, vol. 10, pp. 1789-1795, 2015.

49. B. Pilicheva, M. Draganova-Filipova, and P. Zagorchev, et al., "Invetigation of betahistine dihydrochloride biocompatibility and nasal permeability *in vitro*," *Journal of Applied Biomedicine*, vol. 14, pp. 299-305, 2016.

50. M. James, Anderson, and M. Christina Van Itallie, "Physiology and Function of the Tight Junction," *Cold Spring Harbor Perspectives in Biology*, vol. 1.2, 2009.

51. A. E. Farkas, C. T. Capaldo, and A. Nusrat, "Regulation of epithelial proliferation by tight junction proteins," *Annals of the New York Academy of Sciences*, vol. 1258, pp. 115–124, 2012.

52. P. J. Sikora, D. Chlebna-Sokół and A. Krzyzańska-Oberbek, "Proinflammatory cytokines (IL-6, IL-8), cytokine inhibitors (IL-6sR, sTNFRII) and anti-inflammatory cytokines (IL-10, IL-13) in the pathogenesis of sepsis in newborns and infants," *Archivum immunologiae et therapiae experimentalis*, vol. 49, pp. 399-404, 2001.

53. P. K. Jeffery, "Pathological spectrum of airway inflammation. Cellular Mechanisms in Airways Inflammation," *Progress in Inflammation Research*, Birkhauser Verlag. pp. 1–52.

2001.

54. C. D. Douillet, W. P. Robinson, and P. M. Milano, et al., "Nucleotides Induce IL-6 Release from Human Airway Epithelia via $P2Y_2$ and p38 MAPK-Dependent Pathways," *Am J Physiol Lung Cell Mol Physiol*, vol. 291, pp. 734–746, 2006.

55. C. B. Wang, C. K. Wong, and W. K. Ip, et al., "Induction of IL-6 in co-culture of bronchial epithelial cells and eosinophils is regulated by p38 MAPK and NF-kappaB," *Allergy*, vol. 60, pp. 1378–1385, 2005.

56. P. C. Heinrich, J. V. Castell, and T. Andus, "Interleukin-6 and the acute phase response," *Biochem J*, vol. 265, pp. 621–636, 1990.

57. T. Tanaka, M. Narazaki, and T. Kishimoto, "IL-6 in Inflammation, Immunity, and Disease." *Cold Spring Harbor Perspectives in Biology*, vol. 6.10, 2014.

58. Y. Sun, F. Wu, and F. Sun, et al., "Adenosine promotes IL-6 release in airway epithelia," *J Immunol*, vol. 180, pp. 4173–4181, 2008.

59. A. Chow, J. Liang, and J. Wong, et al., "Polarized Secretion of Interleukin (IL)-6 and IL-8 by Human Airway Epithelia 16HBE14o- Cells in Response to Cationic Polypeptide Challenge," *PLoS ONE*, vol. 5(8), 2010.

60. A. Sydbom, A. Blomberg, and S. Parnia, et al., "Health effects of diesel exhaust emissions," *Eur Respir J*, vol. 17(4), pp. 733–46, 2001.

61. I. Tomasek, C. J. Horwell, and D. E. Damby, et al., "Combined exposure of diesel exhaust particles and respirable Soufriere Hills volcanic ash causes a (pro-)inflammatory response

in an *in vitro* multicellular epithelial tissue barrier model," *Particle and Fibre Toxicology*, vol.13 pp. 67-80, 2016.

국문 초록

미세먼지 세포기전 연구 플랫폼으로써 기도 상피 모사 칩의 개발

최준희

서울대학교 대학원

협동과정 바이오엔지니어링 전공

본 연구의 목표는 새로운 미세유체 세포 배양 기술을 사용하여 기존의 미세먼지 실험모델보다 생리학적 유사성과 효율성 측면에서 우수한 '기도 상피 모사 칩(Airway Epithelium-on-a-Chip)'을 개발하고 미세먼지의 세포기전 연구에 활용하는 것이다. 나아가 기존 연구의 단점을 보완하는 미세먼지 세포 반응 연구 플랫폼으로써 '기도 상피 모사 칩'의 활용 가능성을 확인하고자 하였다. 본 연구에서는 기도 상피의 연속된 배양을 미세유체 칩에 구현하고, 대기 중 미세먼지의 주요 성분 중 하나인 디젤 파티클 (Diesel Exhaust Particles, 이하 DEP)을 개발된 칩에 투여하여 기도 상피의 염증반응을 관찰하였다. 또한 체외 배양된 세포층과 마우스 천식 모델에서의 DEP 반응을 관찰함으로, 개발된 칩의 기능성과 칩 실험 결과의 신뢰성을 검증하고자 하였다.

기도 상피 모사 칩은 이종세포 배양이 가능한 위층, 세포 외 물질 성분이 코팅된 다공성 막, 그리고 세포의 양분이 흐르는 아래층으로 이루어져있으며, 각 층은 PDMS (polydimethylsiloxane)로 제작되었다. 기도 상피 층의 모사를 위해 미세유체 칩의 위 채널에 비강 내피 세포와 폐포 상피 세포가 직렬로 배양되었다. 또한 미세유체 칩 내 세포배양을 돕기 위해 파이브로넥틴이 코팅된 PET (Polyethylene

terephthalate) 막이 사용되었다.

칩 내에 서로 다른 구역에 배양된 두 기도 상피 세포는 모두 채널에 주입된 후 48시간 이내에 온전한 밀착 연결을 형성하였으며, 3-4일 이내에 채널 전체에 증식하여 상피 세포층을 형성하였다. 현미경 이미지 분석을 통해 두 기도 세포가 직렬 공 배양된 것을 확인하였고, 시간에 따른 두 세포들의 생장도 확인하였다. 형성된 세포층에 DEP를 투여한 결과 형성된 밀착 연결이 끊어지는 EMT 현상이 관찰 되었고, 염증 사이토카인의 종류인 IL-6가 증가하는 것을 확인하였다. 동시에 진행된 배양 접시에서의 실험을 통해 DEP 투여 시 세포층의 밀착 연결이 끊어지는 것을 확인하였고, 천식 마우스 모델을 통해 DEP 투여 시 IL-6 사이토카인의 mRNA 발현 정도가 증가하는 것을 확인하였다. 실험 결과, 개발된 미세유체 칩 내에 두 종류의 기도세포가 직렬 공 배양됨을 증명하였고, 칩에서 검출된 DEP 실험 결과가 세포 배양 접시 실험과 동물 실험에서의 결과와 일치함을 확인함으로써 기도 상피 모사 칩의 기능성과 신뢰성을 검증하였다.

본 연구에서 소개된 미세유체 칩 내 이종 세포 배양 기법은 세포의 연속 배양을 실현할 수 있고, 나아가 상피 세포층 간의 상호작용에 대한 연구가 가능하다는 잠재성이 있다. 추가적인 연구로, 개발된 모델의 기능적, 환경적 유사성을 개선하기 위해 혈관 내피 세포의 배양과 일차 세포 (Human primary cells)의 배양 및 분화가 필요하고, 미세먼지 연구의 기능성을 높이기 위해 DEP 외의 다른 미세먼지 후보를 이용한 추가적인 검증이 필요하다. 그럼에도 본 논문은 기도 상피 모사 칩이 미세먼지의 기도 세포 기전 연구의 새로운 플랫폼으로써 활용 될 수 있음을 시사한다.

주요어 (Keywords): 기도상피 모사 칩, 장기 칩, 미세먼지, 디젤 파티클
학번: 2016-21181